Swell and Destroy: A MOF-Containing Polymer Sponge that Immobilises and Catalytically Degrades Nerve Agents

Yaroslav Kalinovskyy,[a] Alexander J. Wright,[a] Jennifer R. Hiscock,[a] Toby D. Watts,[a] Marcus J. Main,[b] Rebecca L. Williams,[b] Nicholas J. Cooper,[b]
Simon J. Holder,[a]* and Barry A. Blight[ac]*

[a]*School of Physical Sciences, University of Kent, Ingram Building, Canterbury, CT2 7NH, UK.*
Email: S.J.Holder@kent.ac.uk

[b]*Defence Science and Technology Laboratory, Porton Down, Salisbury, SP4 0JQ, Wiltshire, UK*

[c]*Department of Chemistry, University of New Brunswick, Fredericton, New Brunswick, E3B 5R5, Canada.*
E-mail: B.Blight@unb.ca

Abstract

Organophosphorus chemical warfare agents function as potent neurotoxins. Whilst the destruction of nerve agents is most readily achieved by hydrolysis, their storage and transport is hazardous; lethal in milligram doses with any spillage resulting in fatalities. Furthermore current decontamination and remediation measures are limited by the need for stoichiometric reagents, solvents and buffered solutions, complicating the process for the treatment of bulk contaminants. Herein, we report a composite polymer material capable of rendering bulk VX unusable by immobilisation within a porous polymer until a MOF catalyst fully hydrolyses the neurotoxin. This is an *all-in-one* capability that minimizes the use of multiple reagents, facilitated by a porous high-internal phase emulsion-based polystyrene monolith housing an

active zirconia MOF catalyst (MOF-808); the porous polymer absorbs and immobilises the liquid agents, while the MOF enables hydrolysis. The dichotomous hierarchy of porous materials facilitates the containment and rapid hydrolysis of VX (> 80% degradation in 8 hours) in the presence of excess of H_2O. This composite can further enable the hydrolysis of neat VX with a reliance on ambient humidity (>95% in 11 days). Potentially, 4.5 kg of the composite can absorb, immobilise and degrade the contents of a standard chemical drum/barrel (208 litres, 55 gallons) of chemical warfare agent. We believe that this composite is the first example of what will be the go-to approach for CWA immobilisation and degradation in the future. Furthermore, we believe that this demonstration of a catalytically reusable absorbent sponge provides a signpost for the development of similar materials where immobilisation of a substrate in a catalytically active environment is desirable.

Introduction

Organophosphorus (OP) nerve agents (NAs; OP-NAs), such as the G and V-series are a class of chemical warfare agents (CWAs) that inhibit the enzyme acetylcholinesterase.[1] The acute toxicity of NAs makes them a devastating weapon when deployed against humans. Bulk decontamination procedures still rely on transport of the liquid CWAs to suitable sites for decontamination. For example, following the use of NAs in the Syrian civil war and Syria's accession to the Chemical Weapons Convention, nations led by the US, were involved in the transport of 1,000 metric tons of chemical warfare agents and precursors to industrial sites in Germany, Finland, the United States, and United Kingdom.[2] Their storage and transport is hazardous; lethal in mg doses, any spillage can result in fatalities. Furthermore, in liquid form, nerve agents can readily be obtained (and potentially used) by pouring, siphoning etc from their storage vessel. The actual decontamination procedures often require bulk solvents

for solubilisation and stoichiometric quantities of reagents to degrade CWAs.[3–5] One potential method of immobilising OP-NAs is by employing poly-high-internal-phase emulsions (pHIPEs), which are a class of highly porous polymers consisting of an internal phase greater than 74% of the total volume of the system.[6,7] Recently, we reported a styrenic pHIPE with a 95% internal phase that was shown to swell a variety of V- and Mustard-series agents producing record high absorption degree (Q) values well in excess of 40, and with minimal leeching of the substrate.[8] Separately, metal-organic frameworks (MOFs) have been shown to be effective degradation catalysts for OP-NAs. MOFs are modular, hybrid structures[9–16] that exhibit ultrahigh porosity.[17–20] Zirconium MOFs have shown much promise as heterogeneous catalysts[21–24] for the hydrolysis of OP contaminants such as dimethyl p-nitrophenylphosphate (DMNP; a known pesticide and NA analogue)[25–31] and V-series NAs.[32–35] Zirconium MOFs such as Nu-1000[36] and MOF-808,[37] which possess a lower linker connectivity than the maximum of 12, have been shown to be the most hydrolytically active. Here we report the marriage of these two approaches in a MOF/pHIPE composite material capable of simultaneously absorbing and degrading the V-series agent VX (diisopropylaminoethyl-*O*-ethyl methylphosphonothioate). Whilst there have been previous reports of MOF-polymer mixtures and composites[38–42] (including examples of MOF-polymers for the degradation of nerve agents) we believe the material described in this paper demonstrates for the first time the combination of an active polymer matrix for the absorption and gelation of bulk organic substrates with a catalyst that can degrade said substrate; a dual purpose functional material. The substituent parts of the composite are a 95 % internal phase (IP) styrene-based pHIPE and the six-connected zirconium MOF-808. The HIPE monolith functions as a swelling absorbent for VX, while in parallel, MOF-808 facilitates the OP substrate's hydrolytic degradation. Absorption experiments were conducted on the CWA simulant methyl benzoate,[43] and initial buffered hydrolysis experiments were performed on the CWA

degradation simulant DMNP.[25] The composite material does not display any appreciable loss in absorption capacity or hydrolysis performance when compared to the individual composite substituents. Upon utilising a true NA, the composite is shown to quickly degrade VX in a non-buffered aqueous medium. Finally, when the composite material was exposed to neat VX, a slow hydrolysis was observed, one that is driven by ambient humidity alone. Once the agent has been fully absorbed, it can be considered contained and thus unusable, making the slow degradation speed less of a concern. Our composite material demonstrates an approach for the bulk absorption, immobilisation and catalytic breakdown of V-series NAs, increasing the safety of the storage and transport of said materials safety and negating the need for additional reagents and solvents in their degradation.

Results

MOF-HIPE composite synthesis. The first composite, MOF-HIPE, was assembled by introducing powdered MOF-808 to a HIPE emulsion during polymer formation. Whilst there have been elegant reports on the application of the MOF UiO-66 as a Pickering emulsion in the synthesis of HIPE polyamide materials[44] the approach taken here was to simply incorporate the MOF as a catalyst in the HIPE monolith; the surfactant was retained in the formulation to provide emulsion stability. The HIPE was composed of 95 mol% styrene, 5 mol% 4-vinyl benzylchloride (VBCl), and crosslinked with 1,4-divinyl benzene (DVB),[17] the resulting HIPE material had an IP fraction of 95 wgt% water. The MOF-808 loading was 25 wgt % relative to the total monomer weight. This mass was chosen to maximise the amount of MOF in the composite without jeopardising the stability of the emulsion.[45]

All samples containing the MOF went to greater than 99% monomer conversion (NMR analysis of the remaining liquid phase after 72 hours) and no powdery/solid residue was evident upon manipulation of the samples. Repeated absorption and swelling, washing and extraction procedures led to no solid residue from the composites indicating that the MOF was incorporated in the HIPEs quantitatively. The crystallinity of MOF-808 MOF-HIPE was retained in composite form, as shown by PXRD (Figure 1a), while MAS ^{1}HNMR confirmed homogeneity of the polymer component and illustrated the remaining presence of initial surfactant (SI, Figure S5). MOF-HIPE materials were also observed through SEM (Figure 1c,d, and SI, Figures S1, S2 and S6 to S9) to have a porous interconnected network stereotypical of a pHIPE with such a high internal phase fraction.[5] EDX elemental analysis was also performed to confirm the presence of zirconium (Figure 1d; and SI, Figures S6 to S9). Notably whilst the EDX results show high density of Zr that were mapped to the large distinct particles of MOF in the SEM (Figure 1d) it is also distributed more evenly throughout the composite – presumably associated with the larger distribution of smaller MOF particles that are not immediately discernible in the SEM images. A second composite was also synthesised containing 5 mol% of 4-vinyl benzylpiperidine monomer[46] (4-VBPP; pHIPE monomer distribution: 90% styrene, 5% VBCl, 5% VBPP with DVB[17]), and the material was denoted MOF-HIPE-VBPP. The basic amine on the 4-VBPP substituent would function as a stoichiometric heterogeneous buffer for aiding OP hydrolysis.[42] Statistical analysis of the pore sizes by SEM was performed on all samples to assess the impact that the inclusion of MOF catalyst had on the porosity of the monolith component. In all three cases where MOF was included the average pore diameters decreased circa three-fold (from over 6 μm to approximately 2 μm, SI Table S3 and Figure S3).

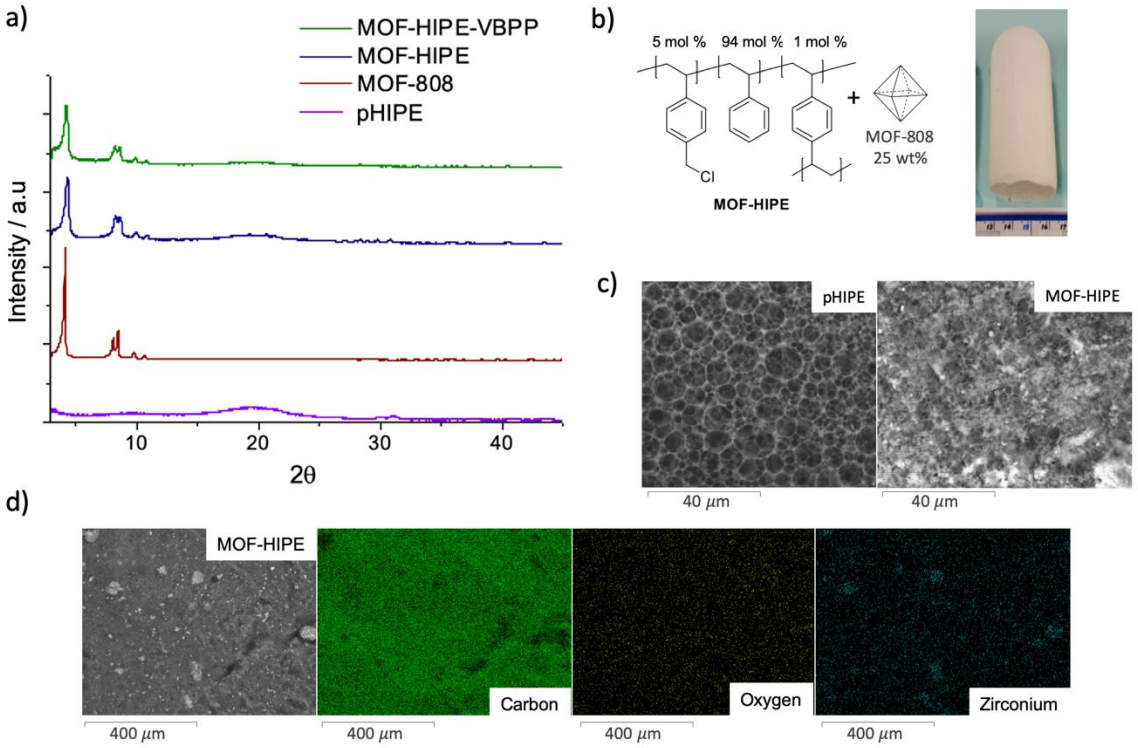

Figure 1. Composite material characterization: **a)** PXRD overlay showing pHIPE, MOF-HIPE and MOF-HIPE-VBPP; **b)** A structural illustration of MOF-HIPE chemical composition and a photograph of a MOF-HIPE monolith. **c)** left to right: electron micrograph of the previously reported 5% VBCl / 95% internal phase pHIPE, electron micrograph showcasing the high porosity of the HIPE membrane in MOF-HIPE; **d)** electron micrograph and elemental mapping (EDX) of MOF-HIPE displaying elemental scans of (left to right) carbon, oxygen, zirconium.

Composite absorption studies. Absorption studies of the composite materials were conducted with methyl benzoate, previously identified as a V-agent simulant for absorption and other physical studies.[43] For each pHIPE, the studies were conducted in triplicate. The following equation was used for calculating Q, the absorption capacity:

$$Q = \frac{(Mass\ of\ swollen\ polymer - mass\ of\ dry\ polymer)}{Mass\ of\ dry\ polymer}$$

Equation 1

Where the HIPE contained additional material such as MOF or surfactant, a modified equation was used for calculating the Q value. This was to offset the additional weight which did not contribute to the swelling. The following modified equation was used:

$$Q_{mod} = \left(\frac{Q}{M_p}\right) * (M_p + M_e) \qquad \textbf{Equation 2}$$

M_p represents the total % mass of the polymer and surfactant, and M_e represents the % mass of the extra components; for example, M_e = 35 in MOF-HIPE (25% MOF and 10% extra surfactant). The absorption (Figure 2a) results are summarized in Figure 2b. MOF-HIPE consisted of a 95% internal phase and an adjusted Q value of 52 was observed, this is comparable to the absorption of the 95% internal phase HIPE which produced a Q value of 55. MOF-HIPE contained additional surfactant and produced the highest adjusted Q value of 63. For the case MOF-HIPE and MOF-HIPE, it can be said that the incorporation of a MOF into the composite structure had no negative impact on the absorption. The addition of the VBPP monomer reduced absorption capacity by roughly 50 % for both HIPE-VBPP (Q = 26) and MOF-HIPE-VBPP (Q = 32). This reason for this effect on absorption is unknown at present and further studies are underway to fully gauge the effect of VBPP inclusion on microstructure and interconnectivity.

To demonstrate that the HIPEs can absorb the DMNP hydrolysis simulant, a qualitative absorption study was performed; MOF-HIPE was shown to readily absorb a 1:3 mixture of DMNP:THF. Despite the strong absorption of organic liquids the HIPEs and the MOF-HIPEs were still able to take up water absorbing 8 to 12 times

their own weight. This is likely due simple capillary action (sponge-like behaviour) though it may be facilitated by the residual surfactant. Contact angle measurements demonstrated that when surfactant was present, the surface of the MOF-HIPE showed more hydrophilicity and water was absorbed. Upon surfactant removal, the resulting composite displayed a water contact-angle of 127.5° and no immediate absorption occurred (Figure 2c).[47]

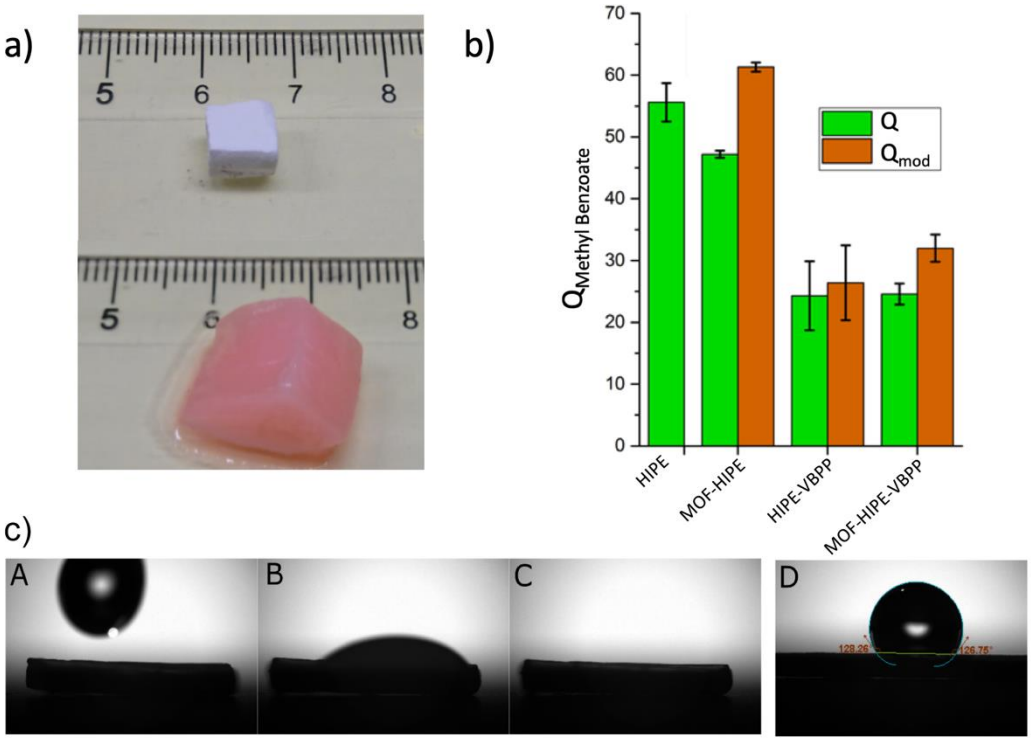

Figure 2. a) Photographs of MOF-HIPE before swelling and at full Q_{mod} > 63 expansion upon exposure to methylbenzoate dyed with crimson Windsor and Newton drawing ink for contrast; **b)** Graph showing the swelling degrees (Q) alongside the Q_{mod} for each of the samples presented in this work. HIPE does not have a Q_{mod} value associated for it as it does not contain any extra components outside of the basic synthesis. **c)** A composite image showing water contact angle measurements recorded at 14 frames per second. A, B and C show a water droplet falling onto the surface of HIPE, there is a difference of two frames

between each image. Image D shows a water droplet on a surfactant free HIPE, no absorption is observed and a hydrophobic contact angle is recorded.[21]

DMNP Simulant Hydrolysis Studies. The performance of the composite materials as hydrolysis catalysts were assessed using DMNP as the substrate, a compound previously identified as a V-agent chemical simulant. All studies were conducted under standardised conditions in the presence of 0.45 M aqueous N-ethyl morpholine (NEM) buffer[25,29] and THF; each experiment was performed in triplicate. THF (Q = 45)[5] was used to dilute DMNP to simulate the viscosity/polarity of VX, thus aiding in the HIPE absorption process. The hydrolysis conditions are noted in Figure 3. In brief, the procedure involved charging an NMR tube with small cubes (typically ~ 1 mm^3) of HIPE polymer (typically ~ 16 mg) containing 1.25 mol% (relative to DMNP) of MOF-808, this was followed by the addition of DMNP. A solution containing THF, H_2O, D_2O and NEM buffer was then added and the tube was immediately placed in an NMR auto-sampler and the reaction followed using ^{31}P NMR spectroscopy by monitoring the appearance of the dimethyl phosphate (DMP) peak (2.8 ppm) relative to the disappearance of DMNP (-4.4 ppm). As expected all reactions were first order with respect to DMNP.[32,36] Spectral data, individual data points and the first order residual plots can all be found in the supporting information (SI, section S3, Figures S10 to S16)). Figure 3a shows a plot of the DMNP hydrolysis giving DMP, in the presence of the composites. No DMNP hydrolysis was observed in the presence of HIPE and HIPE-VBPP due to the lack of MOF catalyst, these materials therefore served as blank control samples. MOF-HIPE (k = 0.0192 s^{-1}) and MOF-HIPE-VBPP (k = 0.0261 s^{-1}) both performed faster than powdered MOF-808 (k = 0.0034 s^{-1}) due to the superior dispersion provided by the high volume HIPE scaffold. In this study, the

powdered MOF-808 was left undisturbed throughout the reaction period. There was a slight difference in the initial hydrolysis rates between MOF-HIPE-VBPP and MOF-HIPE but both reached the same 94-95% hydrolysis after 5 hours.

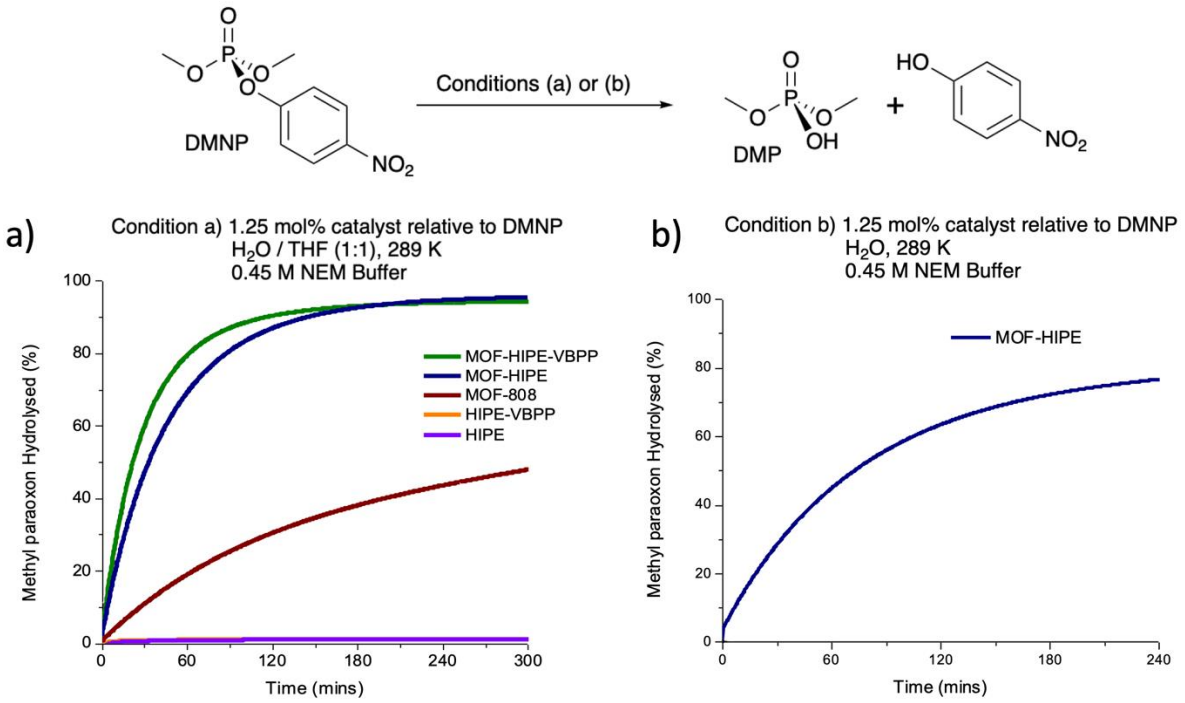

Figure 3. Composite simulant hydrolysis studies as monitored by ^{31}P NMR at 298 K; analysis of the evolution of the DMP peak (2.8 ppm) relative to DMNP (-4.4 ppm): *Condition (a)* A plot showing the hydrolysis of DMNP over time in the presence of the various MOF/HIPE composites with 1.25 mol% catalyst (relative to DMNP) in 0.45 M NEM buffer, THF / H_2O/D_2O (2:1:1). Each set of data was obtained in triplicate and an exponential fit was calculated for each set, plot is therefore an average of three exponential fits;

To validate that the hydrolysis of DMNP was occurring throughout the MOF-HIPE polymer matrix and not simply restricted to surface bound MOF-808, a DMNP hydrolysis experiment was performed to determine the degree of hydrolysis occurring throughout different sections of a cylindrical section of the material. (SI, section 3, Figure S18) over 3 hours. No difference in DMNP hydrolysis was observed between

the inner and outer section of the composite sample (96 and 97% hydrolysis respectively) and significantly less hydrolysis product was present in the reaction supernatant (16% hydrolysis).. Secondly, to confirm the reusability of MOF-HIPE, we performed three catalysis cycles using our THF/H_2O and DMNP screening procedure. Between cycles, repeated swelling and vacuum filtration using THF facilitated the extraction of residual reaction products. We achieved 99% hydrolysis, followed by 98% and 89% for the 1st, 2nd and 3rd cycles, respectively (SI, Figure S19). Finally, a non NEM buffered degradation procedure was utilized for DMNP hydrolysis in the presence of the composites. Slow and incomplete hydrolysis was observed in the presence of all composites (see SI: section S3, Table S3). MOF-HIPE-VBPP exhibited the greatest degree of DMNP hydrolysis (46% after 20 hours), thus showcasing the added benefit of the heterogeneous amine buffer.

Aqueous, buffer-free VX hydrolysis.

MOF-HIPE and MOF-HIPE-VBPP were selected for further testing on the NA VX, along with HIPE-VBPP, which would serve as a blank. VX hydrolysis conditions, along with possible hydrolysis products, are illustrated in Figure 4a. To replicate the conditions for DMNP hydrolysis, an NMR tube was charged with VX followed by the addition of a diced HIPE containing 1.25 mol% MOF-808 (relative to VX). A solution of H_2O and THF was then then added to the tube along with a small amount of D_2O, the tube was immediately placed in an NMR auto-sampler. The reaction followed by ^{31}P NMR spectroscopy by observing the evolution of the ethyl methylphosphonic acid (EMPA) peak (25.4 ppm) relative to VX (58.6 ppm). There are two possible hydrolysis products for VX, EMPA (which is relatively benign) and EA-2192 (Figure 4) which exhibits comparable toxicity to VX.[48,49] As expected the absence of a signal at ~40 ppm (due to EA-2192;[22] Figure 4) in the ^{31}P spectrum (see SI: section S3) demonstrated that this by-product was not produced. Figure 4a shows a

plot of the observed degree of VX hydrolysis with time, in the presence of the composites. Minimal hydrolysis was observed in the presence of HIPE-VBPP due to the absence of MOF catalyst. VX hydrolysis was observed in the presence of MOF-HIPE (k = 0.0044 s^{-1}) and MOF-HIPE-VBPP (k = 0.0059 s^{-1}). These results agreed with the buffered DMNP hydrolysis tests where MOF-HIPE-VBPP slightly outperforms MOF-HIPE. Both composites yield a VX half-life ($t_{1/2}$) of approximately 2 hours, revealing a turnover frequency (TOF) of 40 h^{-1}, the highest of any catalytic composite to date.[42]

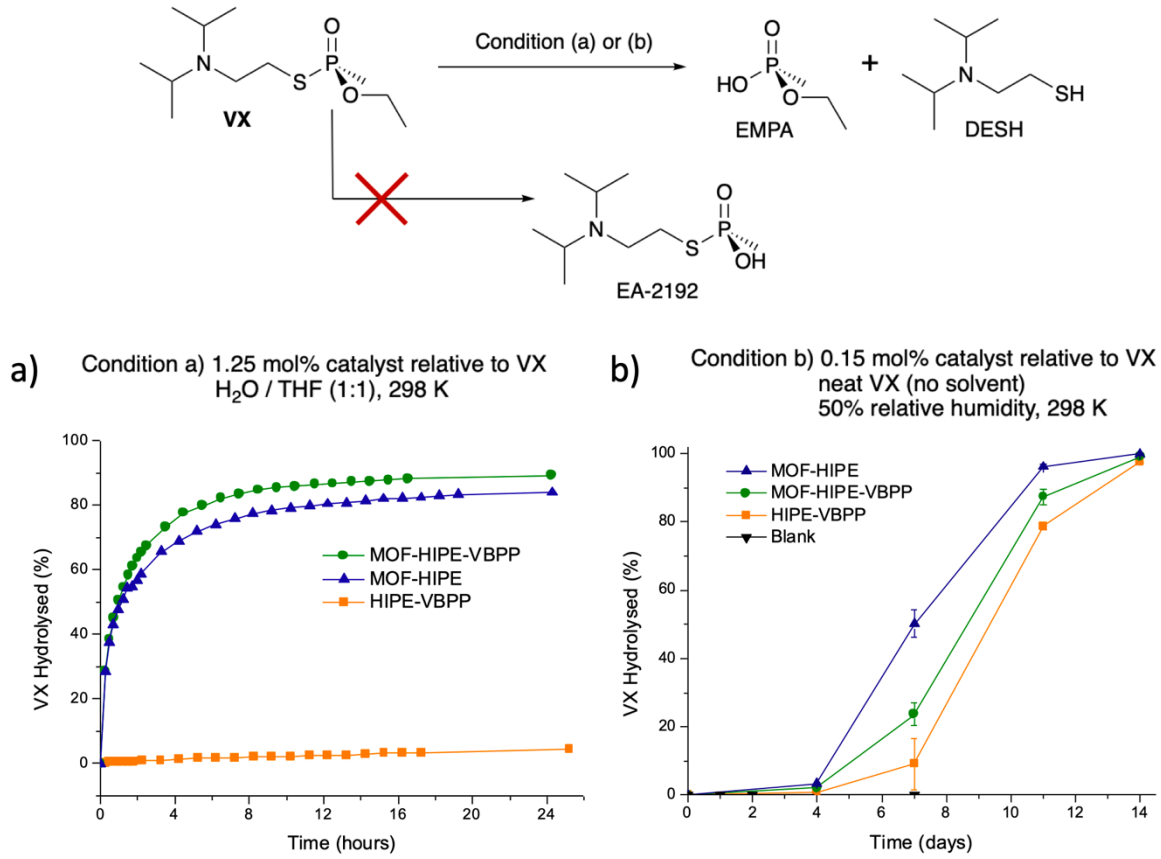

Figure 4. Composite VX hydrolysis studies as monitored with ^{31}P NMR at 298 K; analysis of the evolution of the EMPA peak (25.4 ppm) relative to VX (58.6 ppm). *Condition (a)* A plot showing the hydrolysis of VX over time in the presence of MOF-HIPE-VBPP and MOF-HIPE composites with 1.25 mol% catalyst (relative to VX) in THF / H_2O (1:1). Each set of data was obtained once. *Condition (b)* A plot showing the % degradation of VX over 14 days

by itself (blank) and in the presence of HIPE-VBPP, MOF-HIPE-VBPP and MOF-HIPE with 0.15 mol% catalyst (relative to neat VX) and 50% relative humidity. The error bars show the degree of error observed for the duplicate results.

Neat VX hydrolysis. MOF-HIPE, MOF-HIPE-VBPP and HIPE-VBPP were tested for their ability to degrade neat VX (Figure 4b). The proportion of VX was adjusted to drive the HIPE swelling to Q > 25, this equated to a MOF-808 catalyst loading of just 0.15% relative to VX. The reactions were conducted in open vials to facilitate atmospheric water access (maintained at 50% humidity) to the HIPE composites, and samples were taken at an interval of 4, 7, 11 and 14 days and analysed using ^{31}P NMR, (in duplicate) (see SI: section S4). Minimal hydrolysis was observed after 4 days but after a week, 50% hydrolysis was observed in the presence of MOF-HIPE with near full hydrolysis being achieved after 2 weeks in the presence of all the HIPEs (Figure 4b). When compared to MOF-HIPE-VBPP, MOF-HIPE possesses a significantly superior absorption capacity, and likely enhances access of VX and H_2O to the MOF-808 catalyst housed within. In the case of HIPE-VBPP, we posit that the piperidinyl-buffer facilitates the ambient, organo-catalysed degradation of VX, supported by previous studies assessing the degradation of simulants for the NA Tabun.[50] However, a modest enhancement in VX hydrolysis was observed in the presence of MOF-HIPE-VBPP over that of HIPE-VBPP which can be attributed to the MOF-808 catalyst. The catalytic loading of the MOF-808 catalyst is only 0.15% (relative to VX), showing the significance of this small enhancement. Regardless, MOF-HIPE is shown to be the most effective composite for the complete degradation of neat VX under ambient humidity due to its uptake capacity (Q > 45) and catalytic ability. This is particularly

noteworthy considering that over the same period in the presence of 2% H_2O by mass, without catalysts, the hydrolysis of VX only proceeds to 50% completion.[51]

Conclusions

To summarise, we show that by combining the leading nerve agent absorption agent (styrene pHIPE) along with a MOF hydrolysis catalyst (MOF-808), a styrene-based MOF-HIPE composite can be formed. The resulting material is capable of rendering VX unusable by absorption and immobilisation of the agent within the porous polymer, followed by hydrolytic breakdown catalysed by the MOF. The composite containing a MOF-808 loading of 1.25 mol% relative to VX, was shown to quickly degrade VX in the presence of an excess of water ($t_{1/2}$ < 1 hour). Furthermore the composite was shown to facilitate the absorption and hydrolysis of neat VX in the presence of only ambient humidity ($t_{1/2}$ ~ 7 days). In addition the functional pHIPE material HIPE-VBPP showed interesting amine-centred hydrolysis, and is an area of research we are now pursuing in more detail. The studies described in this work also advance the development of functional materials for the containment and catalytic degradation of other bulk OP contaminants, including both pesticidal analogues of DMNP and other related OP-based NAs. We believe that this demonstration of a catalytically reusable absorbent sponge provides an avenue for the development of similar materials where immobilisation of a substrate in a catalytically active environment is desirable.

References

(1) Delfino, R. T.; Ribeiro, T. S.; Figueroa-Villar, J. D. Organophosphorus Compounds as Chemical Warfare Agents: A Review. *J. Braz. Chem. Soc.* **2009**, *20* (3), 407–428 DOI: 10.1590/S0103-50532009000300003.

(2) Mauroni, Albert, J. Eliminating Syria's Chemical Weapons. *Counterproliferation Pap. Warf. Ser.* **27AD**, No. 58, 1–61.

(3) Yang*, Y.-C. Chemical Detoxification of Nerve Agent VX. **1998** DOI: 10.1021/AR970154S.

(4) Jang, Y. J.; Kim, K.; Tsay, O. G.; Atwood, D. A.; Churchill, D. G. Update 1 of: Destruction and Detection of Chemical Warfare Agents. *Chem. Rev.* **2015**, *115* (24), PR1–PR76 DOI: 10.1021/acs.chemrev.5b00402.

(5) Kim, K.; Tsay, O. G.; Atwood, D. A.; Churchill, D. G. Destruction and Detection of Chemical Warfare Agents. *Chem. Rev.* **2011**, *111* (9), 5345–5403 DOI: 10.1021/cr100193y.

(6) Silverstein, M. S. PolyHIPEs: Recent Advances in Emulsion-Templated Porous Polymers. *Prog. Polym. Sci.* **2014**, *39* (1), 199–234 DOI: 10.1016/J.PROGPOLYMSCI.2013.07.003.

(7) Silverstein, M. S. Emulsion-Templated Porous Polymers: A Retrospective Perspective. *Polymer (Guildf).* **2014**, *55* (1), 304–320 DOI: 10.1016/J.POLYMER.2013.08.068.

(8) Wright, A. J.; Main, M. J.; Cooper, N. J.; Blight, B. A.; Holder, S. J. Poly High Internal Phase Emulsion for the Immobilization of Chemical Warfare Agents. *ACS Appl. Mater. Interfaces* **2017**, *9* (37), 31335–31339 DOI: 10.1021/acsami.7b09188.

(9) Wang, C.; Liu, D.; Lin, W. Metal–Organic Frameworks as A Tunable Platform for Designing Functional Molecular Materials. *J. Am. Chem. Soc.* **2013**, *135* (36), 13222–13234 DOI: 10.1021/ja308229p.

(10) Bitzer, J.; Kleist, W. Synthetic Strategies and Structural Arrangements of Isoreticular Mixed-Component Metal–Organic Frameworks. *Chem. – A Eur. J.* **2019**, *25* (8), 1866–1882 DOI: 10.1002/chem.201803887.

(11) Diercks, C. S.; Kalmutzki, M. J.; Diercks, N. J.; Yaghi, O. M. Conceptual Advances from Werner Complexes to Metal–Organic Frameworks. *ACS Cent. Sci.* **2018**, *4* (11), 1457–1464 DOI: 10.1021/acscentsci.8b00677.

(12) Chen, Z.; Hanna, S. L.; Redfern, L. R.; Alezi, D.; Islamoglu, T.; Farha, O. K. Reticular Chemistry in the Rational Synthesis of Functional Zirconium Cluster-Based MOFs. *Coord. Chem. Rev.* **2019**, *386*, 32–49 DOI: 10.1016/J.CCR.2019.01.017.

(13) Cohen, S. M. Modifying MOFs: New Chemistry, New Materials. *Chem. Sci.* **2010**, *1* (1), 32 DOI: 10.1039/c0sc00127a.

(14) Islamoglu, T.; Goswami, S.; Li, Z.; Howarth, A. J.; Farha, O. K.; Hupp, J. T. Postsynthetic Tuning of Metal–Organic Frameworks for Targeted Applications. *Acc. Chem. Res.* **2017**, *50* (4), 805–813 DOI: 10.1021/acs.accounts.6b00577.

(15) Eddaoudi, M.; Moler, D. B.; Li, H.; Chen, B.; Reineke, T. M.; O'Keeffe, M.; Yaghi, O. M. Modular Chemistry: Secondary Building Units as a Basis for the Design of Highly Porous and Robust Metal−Organic Carboxylate Frameworks. *Acc. Chem. Res.* **2001**, *34* (4), 319–330 DOI: 10.1021/ar000034b.

(16) Guillerm, V.; Kim, D.; Eubank, J.; … R. L.-C. S.; 2014, undefined. A Supermolecular Building Approach for the Design and Construction of Metal–Organic Frameworks.

pubs.rsc.org.

(17) Senkovska, I.; Kaskel, S. Ultrahigh Porosity in Mesoporous MOFs: Promises and Limitations. *Chem. Commun.* **2014**, *50* (54), 7089 DOI: 10.1039/c4cc00524d.

(18) Liu, D.; Zou, D.; Zhu, H.; Zhang, J. Mesoporous Metal-Organic Frameworks: Synthetic Strategies and Emerging Applications. *Small* **2018**, *14* (37), 1801454 DOI: 10.1002/smll.201801454.

(19) Furukawa, H.; Ko, N.; Go, Y. B.; Aratani, N.; Choi, S. B.; Choi, E.; Yazaydin, A. Ö.; Snurr, R. Q.; O'Keeffe, M.; Kim, J.; Yaghi, O. M. Ultrahigh Porosity in Metal-Organic Frameworks. *Science (80-.).* **2010**, *329* (5990), 424–428 DOI: 10.1126/SCIENCE.1192160.

(20) Samokhvalov, A. Adsorption on Mesoporous Metal-Organic Frameworks in Solution: Aromatic and Heterocyclic Compounds. *Chem. - A Eur. J.* **2015**, *21* (47), 16726–16742 DOI: 10.1002/chem.201502317.

(21) Rimoldi, M.; Howarth, A. J.; DeStefano, M. R.; Lin, L.; Goswami, S.; Li, P.; Hupp, J. T.; Farha, O. K. Catalytic Zirconium/Hafnium-Based Metal–Organic Frameworks. *ACS Catal.* **2017**, *7* (2), 997–1014 DOI: 10.1021/acscatal.6b02923.

(22) Cohen, S. M.; Zhang, Z.; Boissonnault, J. A. Toward "MetalloMOFzymes": Metal–Organic Frameworks with Single-Site Metal Catalysts for Small-Molecule Transformations. *Inorg. Chem.* **2016**, *55* (15), 7281–7290 DOI: 10.1021/acs.inorgchem.6b00828.

(23) García-García, P.; Müller, M.; Corma, A. MOF Catalysis in Relation to Their Homogeneous Counterparts and Conventional Solid Catalysts. *Chem. Sci.* **2014**, *5* (8), 2979 DOI: 10.1039/c4sc00265b.

(24) Yoon, M.; Srirambalaji, R.; Kim, K. Homochiral Metal–Organic Frameworks for Asymmetric Heterogeneous Catalysis. *Chem. Rev.* **2012**, *112* (2), 1196–1231 DOI: 10.1021/cr2003147.

(25) Katz, M. J.; Mondloch, J. E.; Totten, R. K.; Park, J. K.; Nguyen, S. T.; Farha, O. K.; Hupp, J. T. Simple and Compelling Biomimetic Metal-Organic Framework Catalyst for the Degradation of Nerve Agent Simulants. *Angew. Chemie Int. Ed.* **2014**, *53* (2), 497–501 DOI: 10.1002/anie.201307520.

(26) Dwyer, D. B.; Dugan, N.; Hoffman, N.; Cooke, D. J.; Hall, M. G.; Tovar, T. M.; Bernier, W. E.; DeCoste, J.; Pomerantz, N. L.; Jones, W. E. Chemical Protective Textiles of UiO-66-Integrated PVDF Composite Fibers with Rapid Heterogeneous Decontamination of Toxic Organophosphates. *ACS Appl. Mater. Interfaces* **2018**, *10* (40), 34585–34591 DOI: 10.1021/acsami.8b11290.

(27) Dwyer, D. B.; Lee, D. T.; Boyer, S.; Bernier, W. E.; Parsons, G. N.; Jones, W. E. Toxic Organophosphate Hydrolysis Using Nanofiber-Templated UiO-66-NH_2 Metal–Organic Framework Polycrystalline Cylinders. *ACS Appl. Mater. Interfaces* **2018**, *10* (30), 25794–25803 DOI: 10.1021/acsami.8b08167.

(28) Bůžek, D.; Demel, J.; Lang, K. Zirconium Metal–Organic Framework UiO-66: Stability in an Aqueous Environment and Its Relevance for Organophosphate Degradation. *Inorg. Chem.* **2018**, *57* (22), 14290–14297 DOI: 10.1021/acs.inorgchem.8b02360.

(29) de Koning, M. C.; van Grol, M.; Breijaert, T. Degradation of Paraoxon and the Chemical Warfare Agents VX, Tabun, and Soman by the Metal–Organic Frameworks UiO-66-NH_2 , MOF-808, NU-1000, and PCN-777. *Inorg. Chem.* **2017**, *56* (19),

11804–11809 DOI: 10.1021/acs.inorgchem.7b01809.

(30) Li, P.; Klet, R. C.; Moon, S.-Y.; Wang, T. C.; Deria, P.; Peters, A. W.; Klahr, B. M.; Park, H.-J.; Al-Juaid, S. S.; Hupp, J. T.; Farha, O. K. Synthesis of Nanocrystals of Zr-Based Metal–Organic Frameworks with Csq-Net: Significant Enhancement in the Degradation of a Nerve Agent Simulant. *Chem. Commun.* **2015**, *51* (54), 10925–10928 DOI: 10.1039/C5CC03398E.

(31) Liu, Y.; Moon, S.-Y.; Hupp, J. T.; Farha, O. K. Dual-Function Metal–Organic Framework as a Versatile Catalyst for Detoxifying Chemical Warfare Agent Simulants. *ACS Nano* **2015**, *9* (12), 12358–12364 DOI: 10.1021/acsnano.5b05660.

(32) Moon, S.-Y.; Wagner, G. W.; Mondloch, J. E.; Peterson, G. W.; DeCoste, J. B.; Hupp, J. T.; Farha, O. K. Effective, Facile, and Selective Hydrolysis of the Chemical Warfare Agent VX Using Zr_6 -Based Metal–Organic Frameworks. *Inorg. Chem.* **2015**, *54* (22), 10829–10833 DOI: 10.1021/acs.inorgchem.5b01813.

(33) Katz, M. J.; Moon, S.-Y.; Mondloch, J. E.; Beyzavi, M. H.; Stephenson, C. J.; Hupp, J. T.; Farha, O. K. Exploiting Parameter Space in MOFs: A 20-Fold Enhancement of Phosphate-Ester Hydrolysis with UiO-66-NH_2. *Chem. Sci.* **2015**, *6* (4), 2286–2291 DOI: 10.1039/C4SC03613A.

(34) Mondloch, J. E.; Katz, M. J.; Isley III, W. C.; Ghosh, P.; Liao, P.; Bury, W.; Wagner, G. W.; Hall, M. G.; DeCoste, J. B.; Peterson, G. W.; Snurr, R. Q.; Cramer, C. J.; Hupp, J. T.; Farha, O. K. Destruction of Chemical Warfare Agents Using Metal–Organic Frameworks. *Nat. Mater.* **2015**, *14* (5), 512–516 DOI: 10.1038/nmat4238.

(35) Soares, C. V.; Leitão, A. A.; Maurin, G. Computational Evaluation of the Chemical Warfare Agents Capture Performances of Robust MOFs. *Microporous Mesoporous*

Mater. **2019**, *280*, 97–104 DOI: 10.1016/J.MICROMESO.2019.01.046.

(36) Moon, S.-Y.; Liu, Y.; Hupp, J. T.; Farha, O. K. Instantaneous Hydrolysis of Nerve-Agent Simulants with a Six-Connected Zirconium-Based Metal-Organic Framework. *Angew. Chemie Int. Ed.* **2015**, *54* (23), 6795–6799 DOI: 10.1002/anie.201502155.

(37) Kalinovskyy, Y.; Cooper, N. J.; Main, M. J.; Holder, S. J.; Blight, B. A. Microwave-Assisted Activation and Modulator Removal in Zirconium MOFs for Buffer-Free CWA Hydrolysis. *Dalt. Trans.* **2017**, *46* (45) DOI: 10.1039/c7dt03616g.

(38) Li, S.; Huo, F. Metal–Organic Framework Composites: From Fundamentals to Applications. *Nanoscale* **2015**, *7* (17), 7482–7501 DOI: 10.1039/C5NR00518C.

(39) Zhu, Q.-L.; Xu, Q. Metal–Organic Framework Composites. *Chem. Soc. Rev.* **2014**, *43* (16), 5468–5512 DOI: 10.1039/C3CS60472A.

(40) Wang, J.; Zhu, H.; Li, B.-G.; Zhu, S. Interconnected Porous Monolith Prepared via UiO-66 Stabilized Pickering High Internal Phase Emulsion Template. *Chem. - A Eur. J.* **2018**, *24* (61), 16426–16431 DOI: 10.1002/chem.201803628.

(41) Chen, Z.; Islamoglu, T.; Farha, O. K. Toward Base Heterogenization: A Zirconium Metal–Organic Framework/Dendrimer or Polymer Mixture for Rapid Hydrolysis of a Nerve-Agent Simulant. *ACS Appl. Nano Mater.* **2019**, *2* (2), 1005–1008 DOI: 10.1021/acsanm.8b02292.

(42) Moon, S.-Y.; Proussaloglou, E.; Peterson, G. W.; DeCoste, J. B.; Hall, M. G.; Howarth, A. J.; Hupp, J. T.; Farha, O. K. Detoxification of Chemical Warfare Agents Using a Zr_6 -Based Metal-Organic Framework/Polymer Mixture. *Chem. - A Eur. J.* **2016**, *22* (42), 14864–14868 DOI: 10.1002/chem.201603976.

(43) Wright, A. J.; Main, M. J.; Cooper, N. J.; Blight, B. A.; Holder, S. J. Poly High Internal Phase Emulsion for the Immobilization of Chemical Warfare Agents. *ACS Appl. Mater. Interfaces* **2017**, *9* (37), 31335–31339 DOI: 10.1021/acsami.7b09188.

(44) Dong, Y.; Cao, L.; Li, J.; Yang, Y.; Wang, J. Facile Preparation of UiO-66 /PAM Monoliths *via* CO_2 -in-Water HIPEs and Their Applications. *RSC Adv.* **2018**, *8* (56), 32358–32367 DOI: 10.1039/C8RA05809A.

(45) Zhang, B.; Zhang, J.; Liu, C.; Peng, L.; Sang, X.; Han, B.; Ma, X.; Luo, T.; Tan, X.; Yang, G. High-Internal-Phase Emulsions Stabilized by Metal-Organic Frameworks and Derivation of Ultralight Metal-Organic Aerogels. *Sci. Rep.* **2016**, *6* (1), 21401 DOI: 10.1038/srep21401.

(46) Schultz, A. R.; Jangu, C.; Long, T. E. Thermal and Living Anionic Polymerization of 4-Vinylbenzyl Piperidine. *Polym. Chem.* **2014**, *5* (20), 6003–6011 DOI: 10.1039/C4PY00763H.

(47) Law, K.-Y. Definitions for Hydrophilicity, Hydrophobicity, and Superhydrophobicity: Getting the Basics Right. *J. Phys. Chem. Lett.* **2014**, *5* (4), 686–688 DOI: 10.1021/jz402762h.

(48) Eman Ghanem; Yingchun Li; Chengfu Xu, and; Raushel*, F. M. Characterization of a Phosphodiesterase Capable of Hydrolyzing EA 2192, the Most Toxic Degradation Product of the Nerve Agent VX†. **2007** DOI: 10.1021/BI700561K.

(49) Wagner, G. W.; Peterson, G. W.; Mahle, J. J. Effect of Adsorbed Water and Surface Hydroxyls on the Hydrolysis of VX, GD, and HD on Titania Materials: The Development of Self-Decontaminating Paints. *Ind. Eng. Chem. Res.* **2012**, *51* (9), 3598–3603 DOI: 10.1021/ie202063p.

(50) Barba-Bon, A.; Martínez-Máñez, R.; Sancenón, F.; Costero, A. M.; Gil, S.; Pérez-Pla, F.; Llopis, E. Towards the Design of Organocatalysts for Nerve Agents Remediation: The Case of the Active Hydrolysis of DCNP (a Tabun Mimic) Catalyzed by Simple Amine-Containing Derivatives. *J. Hazard. Mater.* **2015**, *298*, 73–82 DOI: 10.1016/J.JHAZMAT.2015.04.083.

(51) Yu-Chu Yang, *; Linda L. Szafraniec; William T. Beaudry; Dennis K. Rohrbaugh; Lawrence R. Procell, and; Samuel, J. B. Autocatalytic Hydrolysis of V-Type Nerve Agents. **1996** DOI: 10.1021/JO9614506.

Electronic Supplementary Information

Swell and Destroy: A MOF-Containing Polymer Sponge that Immobilises and Catalytically Degrades Nerve Agents

Yaroslav Kalinovskyy,[a] Alexander J. Wright,[a] Jennifer R. Hiscock,[a] Toby D. Watts,[a] Marcus J. Main,[b] Rebecca L. Williams,[b] Nicholas J. Cooper,[b]
Simon J. Holder,[a]* and Barry A. Blight[ac]*

[a]*School of Physical Sciences, University of Kent, Ingram Building, Canterbury, CT2 7NH, UK.*
Email: S.J.Holder@kent.ac.uk

[b]*Defence Science and Technology Laboratory, Porton Down, Salisbury, SP4 0JQ, Wiltshire, UK*

[c]*Department of Chemistry, University of New Brunswick, Fredericton, New Brunswick, E3B 5R5, Canada.*
E-mail: B.Blight@unb.ca

Table of Contents

Section 1: General Information

Instrumentation

^{1}H and ^{31}P NMR spectroscopy was conducted using a Bruker NEO 400 MHz spectrometer with an auto-sampler at 298 K and 16 scans per measurement.

PXRD patterns were collected on zero-background sample holder using a Rigaku Miniflex 600 desktop XRD.

Proton HR-MAS NMR were acquired using a Bruker NEO 400 MHz at 295 K. The samples were analysed using a $^{1}H/^{13}C$ HR-MAS semi-solids probe which utilised magic angle spinning (54.736 ^{o}) at a frequency of 5000 Hz. The relaxation delay was set to 60 seconds.

Electron micrographs were gathered using a Hitachi S-3400 scanning electron microscope. The polymer samples were prepared for SEM by drying thoroughly and then cutting into thin slices with care taken to not disrupt or damage the surface of the sample.

Infra-red spectroscopy was carried out on a Shimadzu IRAffinity-1S, with an ATR gate, a sweep of 500 - 4000 cm^{-1}, a resolution of 0.5 cm^{-1} and 64 scans.

Section 2: Synthetic Protocols and Characterisation

Synthesis of MOF-808

Procedure from reference 16 in manuscript. In a 250 ml vessel, $ZrCl_4$, 1281 mg (5.5 mmol) was dissolved in 60 ml of *N,N*-dimethylformamide and sonicated for 10 minutes. 1,3,5-benzenetricarboxylic acid (H_3BTC), 372 mg (1.78mol) was then added and the solution was sonicated for a further 10 minutes. Finally, 31 ml (542mmol) acetic acid was added to the solution which was sonicated for another 10 minutes. The solution was sealed in a glass vial and placed in a preheated oven where it was heated at 130 ^oC for 24 hours. The vial was removed from the oven and allowed to cool to room temperature. A white solid was observed. The solid was vacuum filtered, washed with DMF (3 x 20ml) and acetone (3 x 20 ml). The filtrate was dried under vacuum for 24 hours to yield a white microcrystalline powder of MOF-808.

Synthesis of 4-Vinylbenzyl piperidine

Piperidine (5.8 ml, 5 g, 0.06 mol) was dissolved in 50 ml MeCN. 4-vinylbenzyl chloride (8.5 ml, 9.15 g, 0.06 mol) was then added dropwise to the solution along with a flake of 4-tert-butylcatecholinhibitor. This was followed by the addition of potassium carbonate (16 g, 0.12 mmol). The mixture was refluxed at 120 ^oC for 2 hours. The mixture was subsequently cooled to room temperature and then chilled using an ice bowl and the resulting white precipitate was filtered off and washed with MeCN. Another flake of 4-tert-butylcatechol inhibitor was added to the filtrate. The filtrate was concentrated under reduced pressure to yield a pale-yellow oil which was filtered through an alumina column before use. (8.167 g, 201.30 g/mol, 41 mmol, 69 % yield)

^1H NMR (400 MHz, $CDCl_3$): δ 1.37-1.41 (m, 2H), 1.50-1.56 (m, 4H), 2.33 (m, 4H) 3.42 (s, 2H), 5.18 (d, 1H, J = 10.6 Hz), 5.69 (d, 1H, J = 17.4 Hz), 6.67 (dd, 1H, J = 10.9 Hz, 17.4 Hz), 7.21-7.33 (m, 4H). ^{13}C NMR (CDCl3): δ 24.4, 26.0, 54.5, 63.6, 113.3, 125.9, 129.4, 136.2, 136.7, 138.3.

General procedure for HIPE Formation

The following procedure outlines the general synthesis of a pHIPE, the specific quantities for each formulation can be found in Table S1. The monomers, initiator (AIBN) and surfactant (span-80 (sorbitan monooleate)), were added into a 100ml conical flask. The flask was stirred at 200 rpm with a 4 cm hemispherical PTFE overhead stirred paddle for 5 minutes to homogenize the oil phase. The aqueous phase was then prepared. Potassium sulfate was dissolved into deionized water. In the cases where a MOF was present, this was added into the aqueous solution at a loading of 0.535 g (25 wt % [monomers]), after having been ground by hand to a fine powder. The aqueous phase was then vigorously mixed to suspend the MOF, but not sonicated. This agitation was continued throughout the addition of the aqueous phase to the organic to ensure good homogeneity of the MOF. The stirring speed of the organic mixture was increased to 750 rpm and the aqueous solution was dropped in at rate of around 1 drop per second. After all the aqueous phase was added, the stirring speed was increased further to 1000 rpm and left to homogenize for 5 minutes. The HIPE foam was transferred into a glass container, sealed and cured in an oven at 65 °C for 24 hours. After curing, the pHIPE monoliths were cooled and the vials destroyed to leave two samples of pHIPE. They were then dried under vacuum at 65 °C for 48 hours minimum. For some HIPEs, surfactant was removed by soaking in ethanol for 24 hours followed by filtration and vacuum drying. For pHIPE, MOF-HIPE-S, HIPE-VBPP-S and MOF-HIPE-VBPP-S variants, CHN analysis was conducted to verify inclusion of the piperidinyl functionality (Table S2)

Table S1: A table outlining the feed composition of each pHIPE discussed in this study.

Sample	Styrene g (mmol)	VBC g (mmol)	VBPP g (mmol)	DVB g (mmol)	AIBN g (mmol)	SMO g (mmol)	K_2SO_4 g (mmol)	Water ml
pHIPE	7.509 (72.10)	0.579 (3.79)	n/a	0.099 (0. 760)	0.015 (0.091)	1.65 (3.85)	0.500 (0.287)	155
MOF-pHIPE	1.877 (18.02)	0.145 (0.950)	n/a	0.025 (0. 192)	0.004 (0.024)	0.626 (1.46)	0.130 (0.746)	38.9
pHIPE-VBPP	1.778 (17.10)	0.145 (0.950)	0.191 (0.949)	0.025 (0.192)	0.004 (0.024)	0.626 (1.46)	0.130 (0.746)	39.8
MOF-pHIPE-VBPP	1.778 (17.10)	0.145 (0.950)	0.191 (0.949)	0.025 (0. 192)	0.004 (0.024)	0.0626 (1.46)	0.130 (0.746)	39.8

Table S2. CHN results for pHIPEs and MOF-HIPEs; the pairs of values represent duplicate runs

Sample	%C	%H	%N
HIPE	77.80, 77.84	7.91, 7.85	
MOF-HIPE	71.55, 71.61	7.37, 7.29	
HIPE-VBPP	77.37, 77.27	7.87, 7.95	0.57, 0.54
MOF-HIPE-VBPP	71.96, 72.04	7.35, 7.30	0.42, 0.41

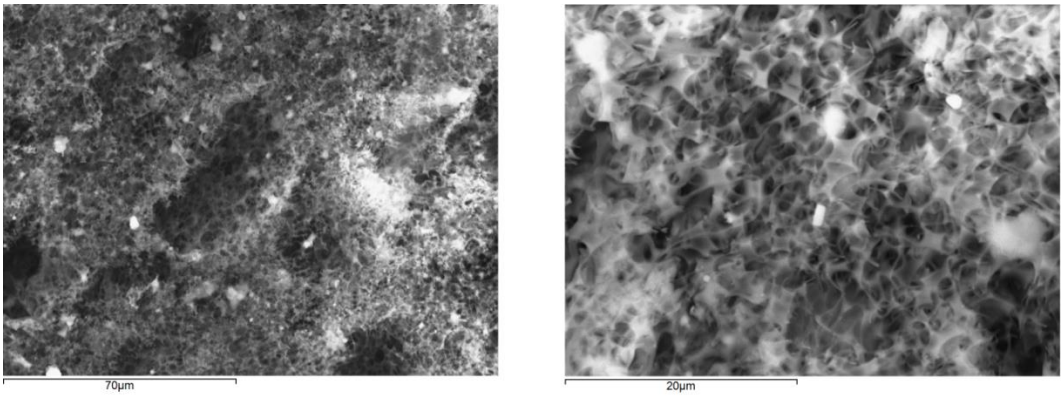

Figure S1. SEM images showing the porous structure of the MOF-HIPE-VBPP membrane and MOF-808 particles embedded in the membrane.

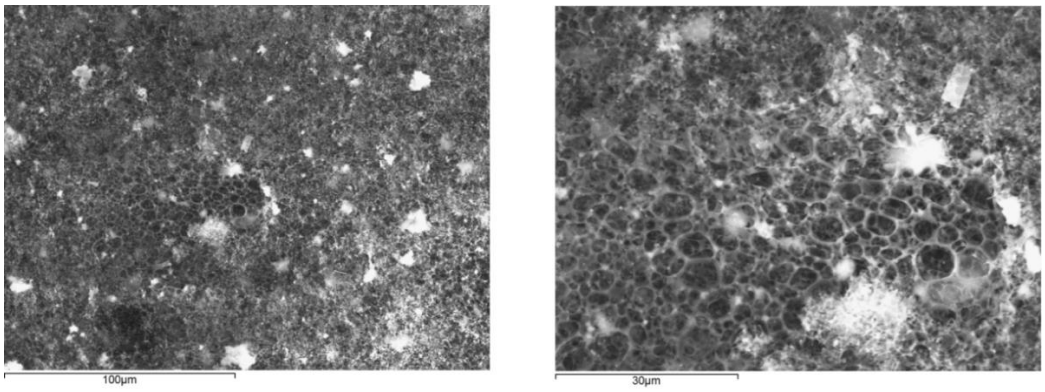

Figure S2. SEM images showing the porous structure of the MOF-HIPE membrane and MOF-808 particles embedded in the membrane.

Table S3. Pore diameter analysis (Image-J anlysis of SEM micrographs) of the composoite materials under investigation.

Sample	Pore diameter μm	Standard deviation μm
pHIPE	6.8	2.0
MOF-HIPE-S	2.3	0.9
MOF-HIPE-VPBB-S	1.6	0.6

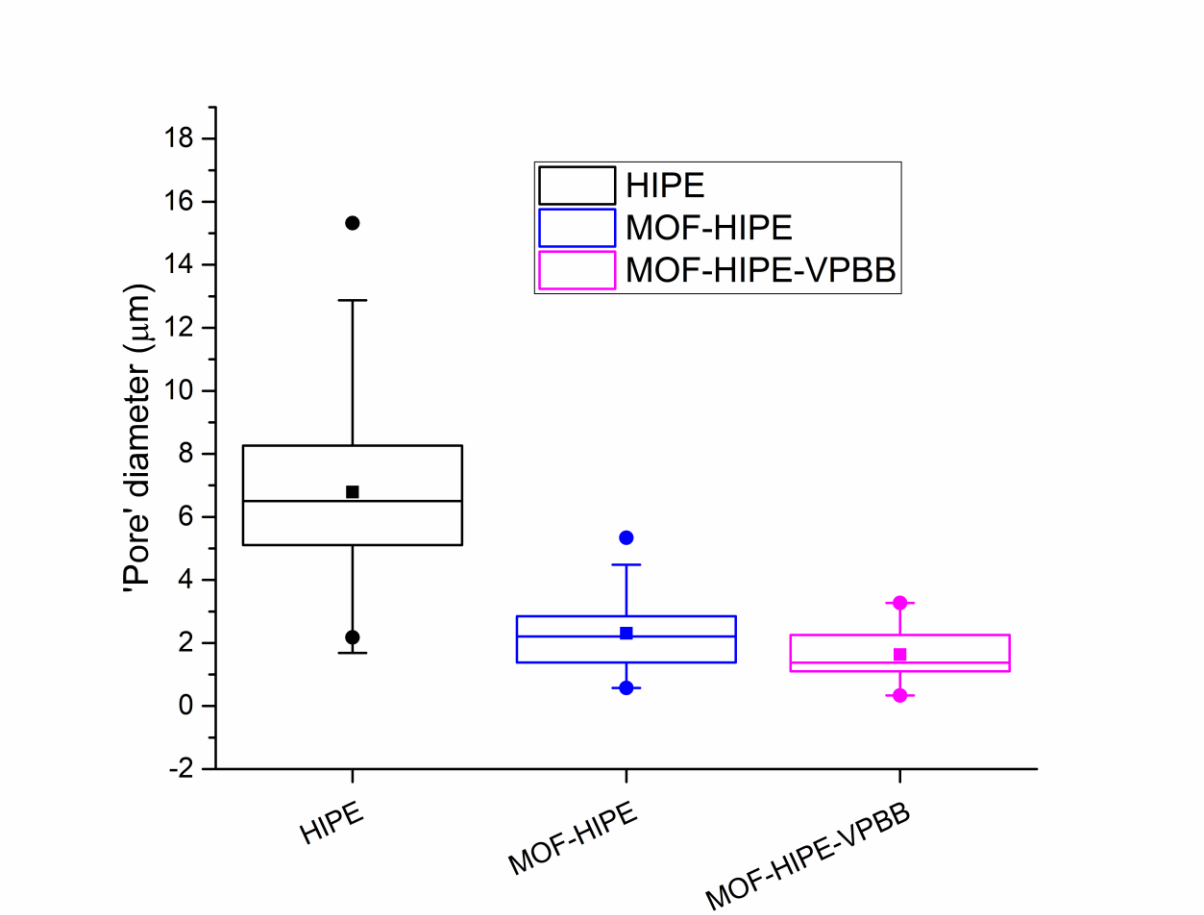

Figure S3. Pore diameter analysis (Image-J anlysis of SEM micrographs) of the composoite materials under investigation.

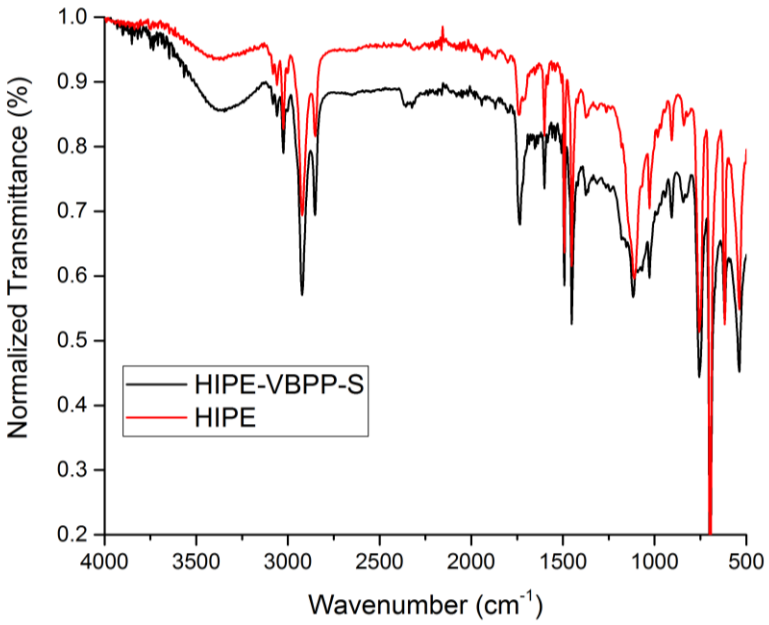

Figure S4. An overlay of the infrared spectra of VBPP-HIPE and HIPE.

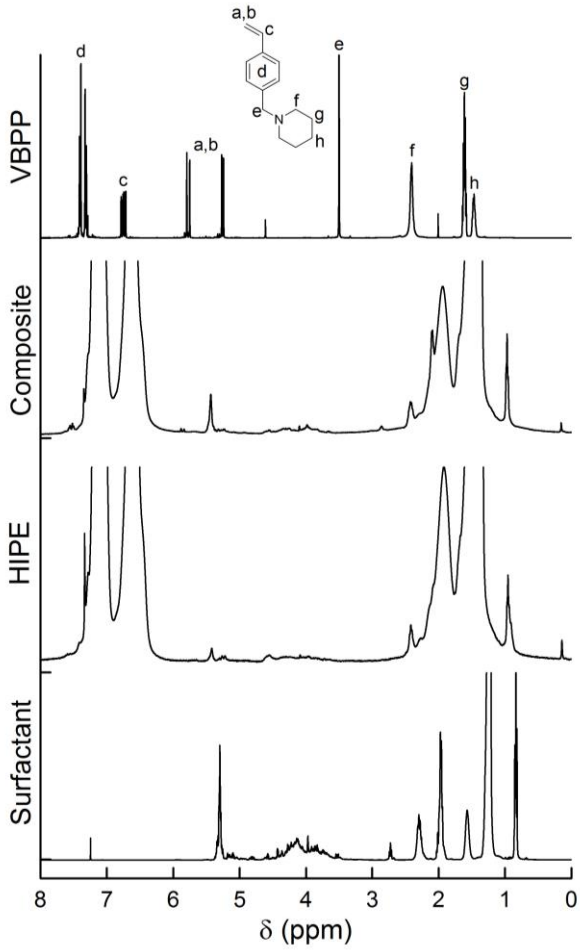

Figure S5. ^{1}H NMR overlay (top to bottom) of VBPP monomer, MOF-HIPE-VBPP, MOF-HIPE and Sorbitan monooleate collected in $CDCl_3$ at 295 K. ^{1}H spectra of MOF-HIPE-VBPP and MOF-HIPE were acquired using HR-MAS NMR.

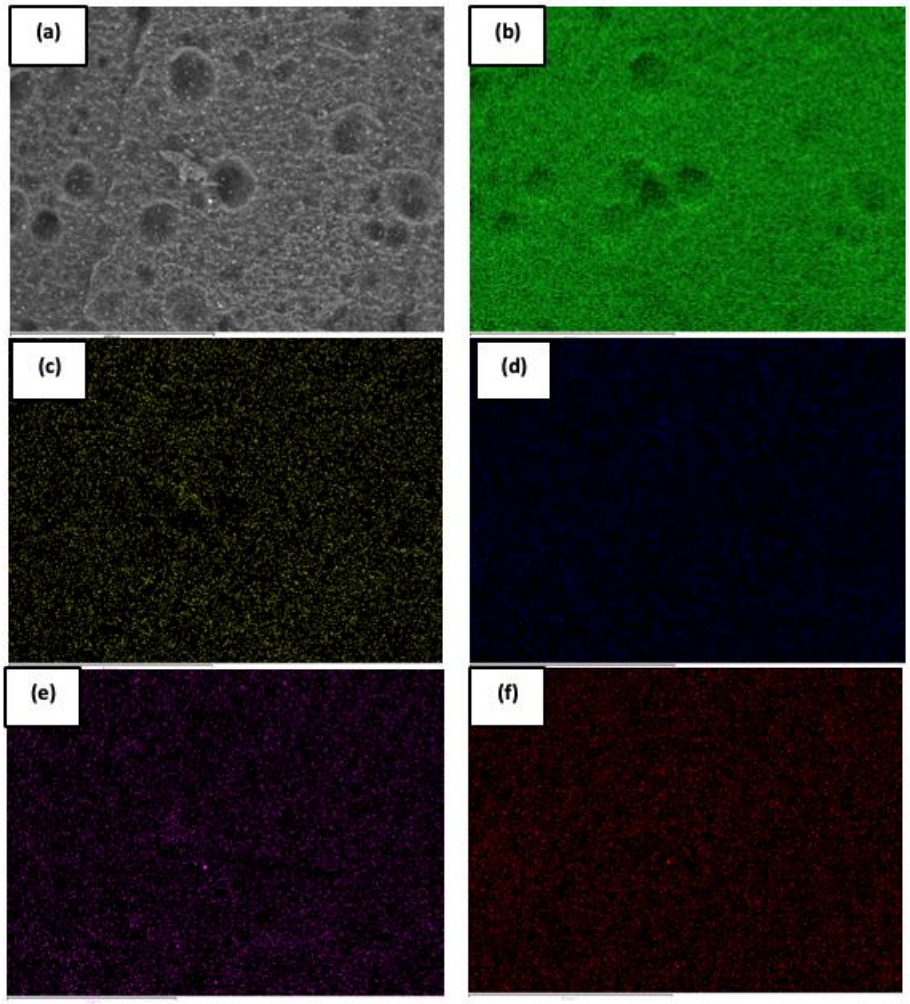

	C	O	S	Cl	K
Average Atomic %	88.19 ± 0.84	10.42 ± 0.82	0.36 ± 0.06	0.37 ± 0.02	0.67 ± 0.11

Figure S6. SEM image of (a) pHIPE; EDS Elemental mapping of (b) carbon, (c) oxygen, (d) sulfur, (e) chlorine and (f) potassium.

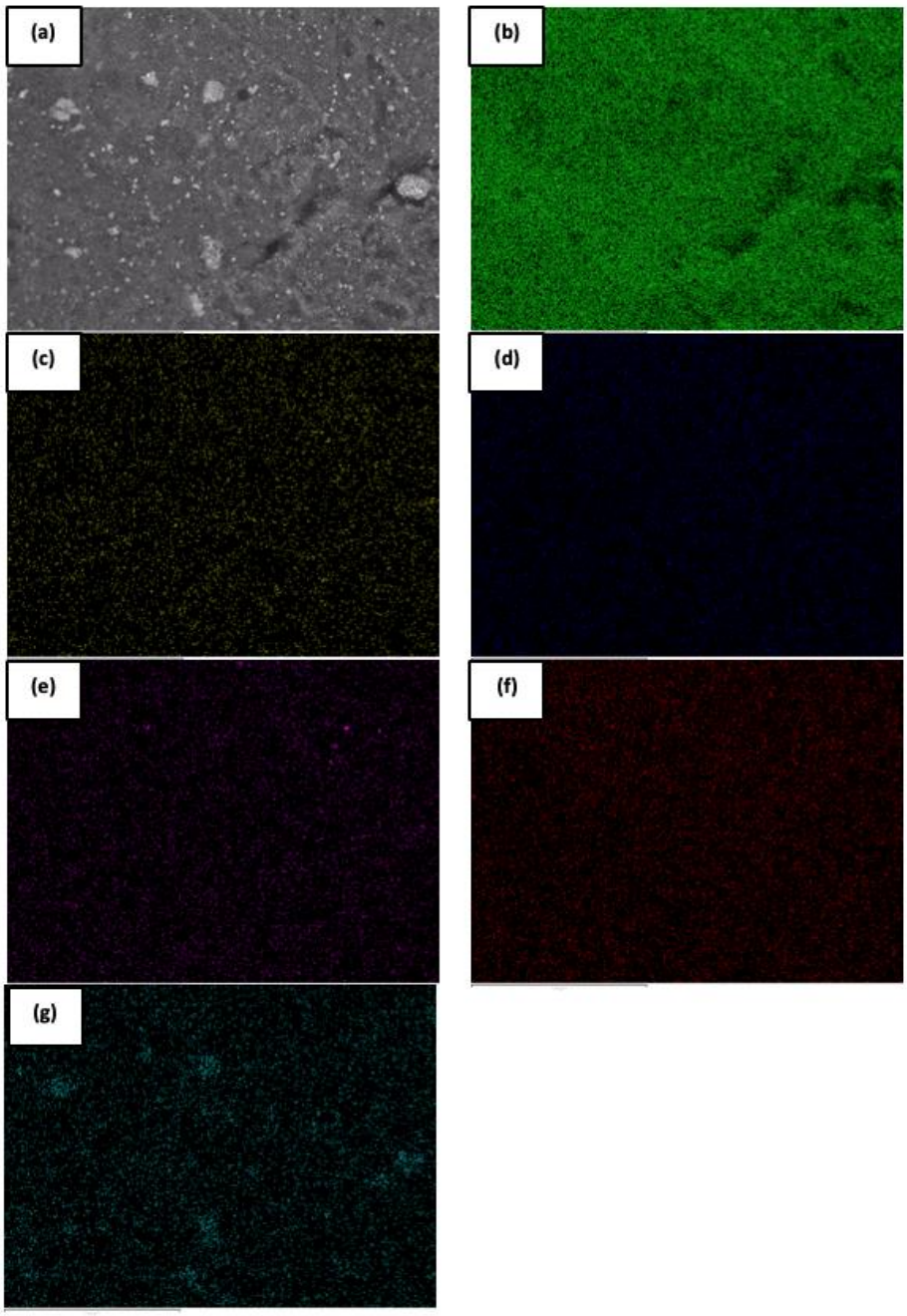

	C	O	S	Cl	K	Zr
Average Atomic %	86.92 ± 1.94	11.39 ± 1.93	0.40 ± 0.01	0.32 ± 0.01	0.76 ± 0.04	0.23 ± 0.02

Figure S7. SEM image of (a) MOF-HIPE- S; EDX elemental mapping of (b) carbon, (c) oxygen, (d) sulfur, (e) chlorine and (f) potassium, and (g) zirconium.

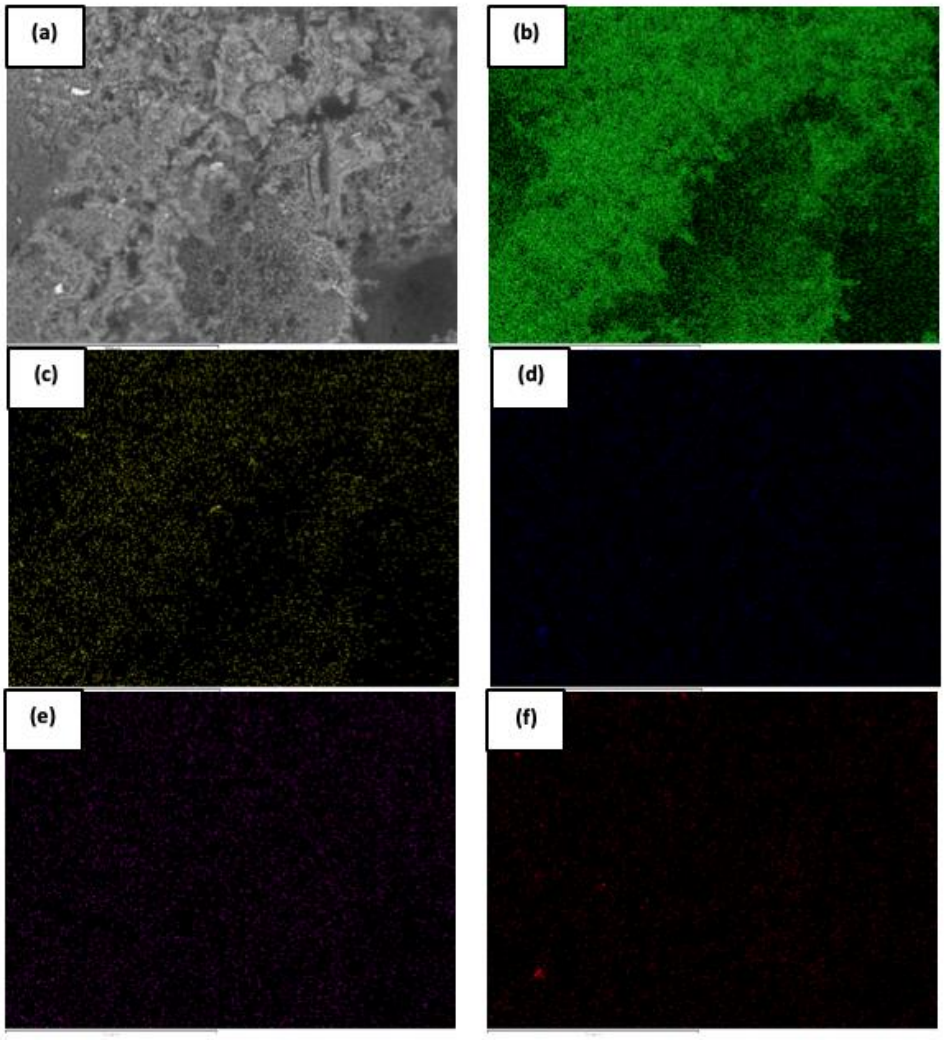

	C	O	S	Cl	K
Average Atomic %	86.07 ± 2.90	12.45 ± 1.28	0.23 ± 0.17	0.52 ± 0.46	0.73 ± 1.02

Figure S8. SEM image of (a) HIPE-VPBB; EDX elemental mapping of (b) carbon, (c) oxygen, (d) sulfur, (e) chlorine and (f) potassium.

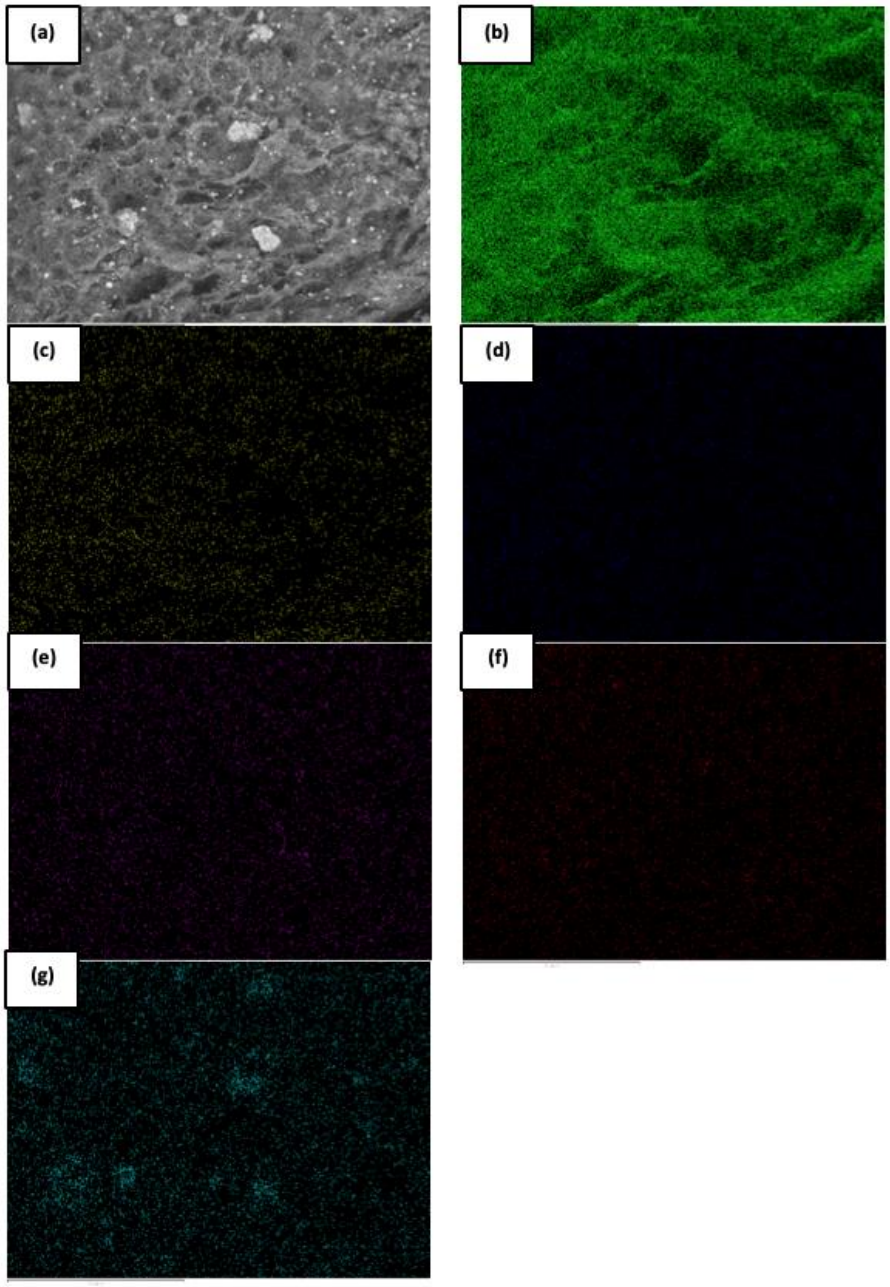

	C	O	S	Cl	K	Zr
Average Atomic %	91.39 ± 0.21	7.78 ± 0.41	0.09 ± 0.02	0.23 ± 0.02	0.15 ± 0.01	0.38 ± 0.15

Figure S9. SEM image of (a) MOF-HIPE-VPBB; EDA elemental mapping of (b) carbon, (c) oxygen, (d) sulfur, (e) chlorine and (f) potassium, and (g) zirconium.

Section 3: Swelling and DMNP Hydrolysis Studies

Swelling procedure with methyl benzoate

A cube of chosen pHIPE composite of mass c. 150 mg submerged in methyl benzoate for 24 hours. The cube was then removed from the methyl benzoate, dabbed onto filter paper and re-weighed. The difference in weight was used to determine the degree of swelling.

Swelling with procedure with water

A cube of chosen pHIPE composite of mass c. 150 mg submerged in water for 24 hours. The cube was then removed from the methyl benzoate, dabbed onto filter paper and re-weighed. The difference in weight was used to determine the degree of swelling.

Table S4. Swelling data of discussed monoliths in water at 298 K.

	HIPE	**MOF-HIPE**	**HIPE-VBPP**	**MOF-HIPE-VBPP**
1	11.11	8.83	4.80	4.90
2	13.70	9.37	3.85	5.56
3	12.60	8.76	6.84	4.85
Average	**12.47**	**8.99**	**5.16**	**5.10**
St. deviation	**1.30**	**0.33**	**1.53**	**0.40**

Buffered DMNP hydrolysis procedure

The following procedure was used to probe the hydrolysis rates of the various MOF and polymer composite materials using a buffered simulant screening system. The HIPE containing MOF-808 (3.2 mg, 0.11 µmol, 1.25 mol %) was sliced up into small pieces (1-2 mm^3) then added to an NMR tube along with DMNP, 20 µL (0.09 mmol). A 0.6 ml mixture containing: 0.2 ml of D_2O, 0.2 THF and 0.2 ml of 1.45 M *N*-ethyl morpholine (NEM) aqueous buffer (effective concentration 0.45 M) was then added to the tube. The tube was inverted once and immediately loaded into an NMR auto-sampler and the first spectrum was obtained within 8-9 minutes of the reaction commencing. The sample was then cycled on the auto-sampler to collect subsequent data points. Each measurement was performed in triplicate (Figure S10-S16).

For the THF-free experiments, the same procedure was followed with the exception of the 0.2 ml of THF being replaced with an additional 0.2 ml of H_2O (Figure S14-17).

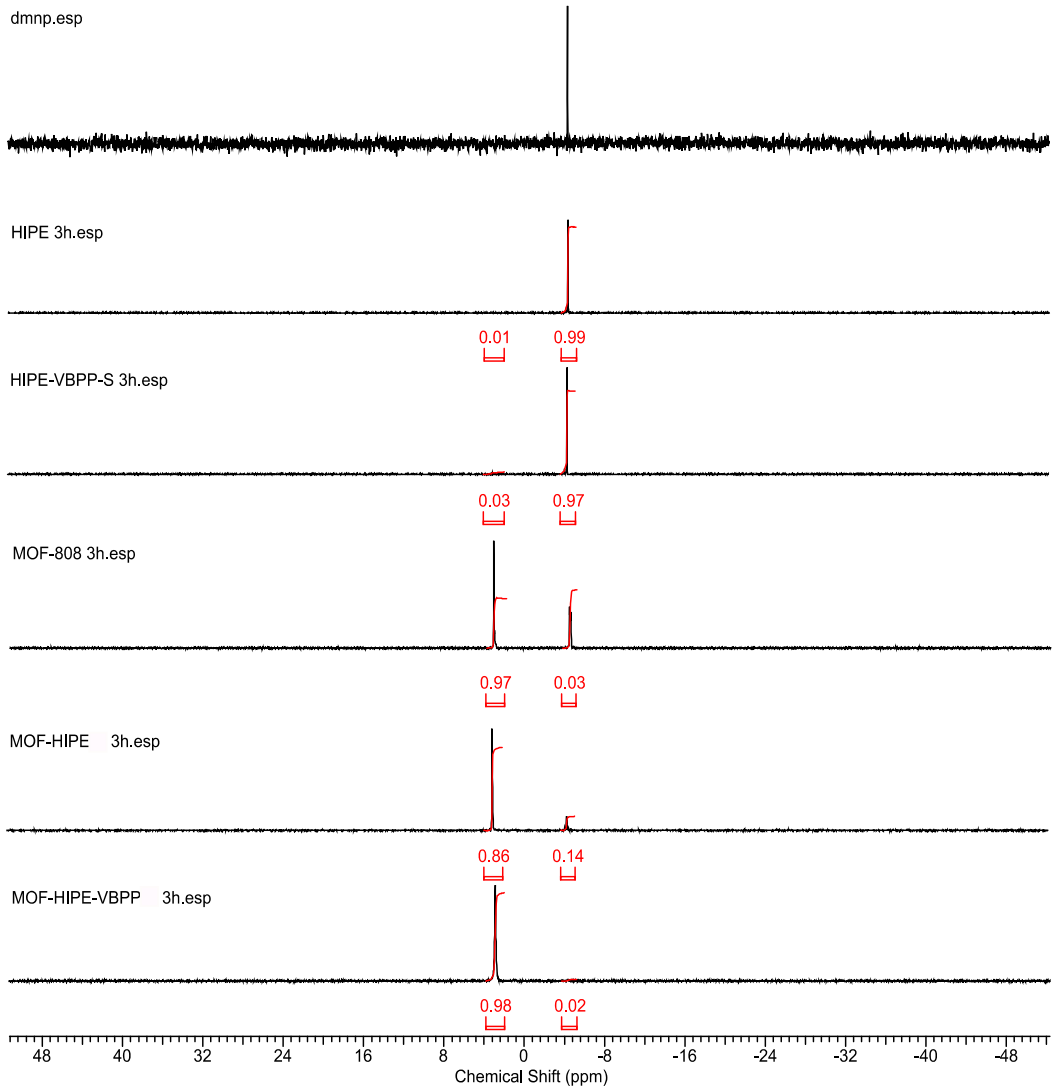

Figure S10. A ^{31}P NMR in D_2O/THF overlay showing DMNP 3 hours after the addition of a corresponding composite/control material in 0.45 M NEM Buffer. The peak at -4.4 pmm is DMNP, the peak at 2.8 ppm is DMP, the DMNP hydrolysis product.

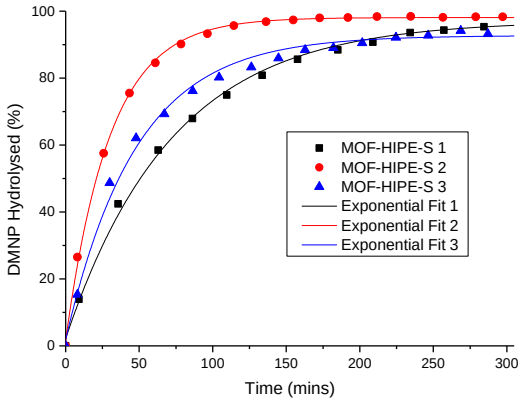

Figure S11. A plot showing the hydrolysis of DMNP over time in the presence of MOF-HIPE with 0.45 M NEM buffer, THF and H_2O. The individual data points for each data set in a triplicate are shown, along with the exponential fit that was derived from each data set.

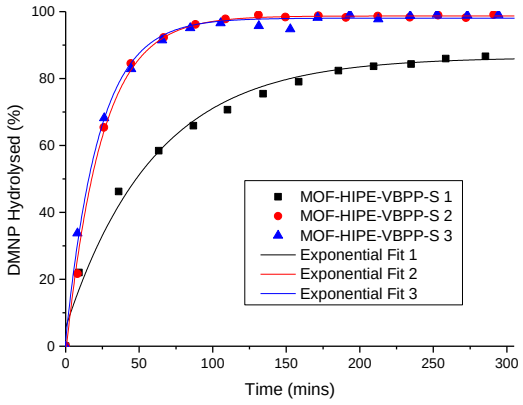

Figure S12. A plot showing the hydrolysis of DMNP over time in the presence of MOF-HIPE-VBPP and 0.45 M NEM buffer, THF and H_2O. The individual data points for each data set in a triplicate are shown, along with the exponential fit that was derived from each data set.

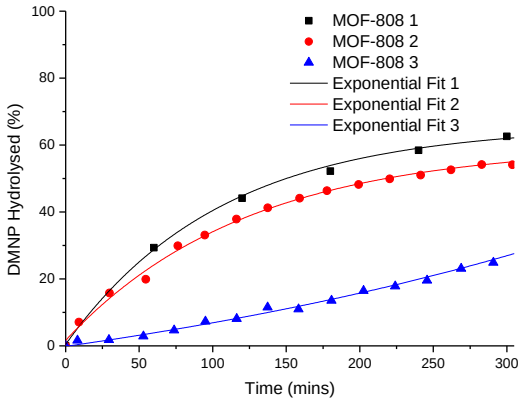

Figure S13. A plot showing the hydrolysis of DMNP over time in the presence of MOF-808 and 0.45 M NEM buffer, THF and H_2O. The individual data points for each data set in a triplicate are shown, along with the exponential fit that was derived from each data set.

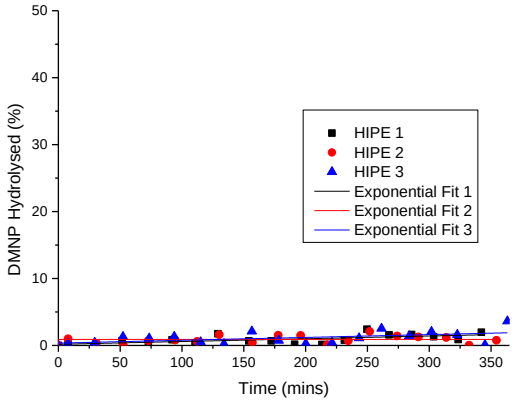

Figure S14. A plot showing the hydrolysis of DMNP over time in the presence of HIPE and 0.45 M NEM buffer, THF and H_2O. The individual data points for each data set in a triplicate are shown, along with the exponential fit that was derived from each data set.

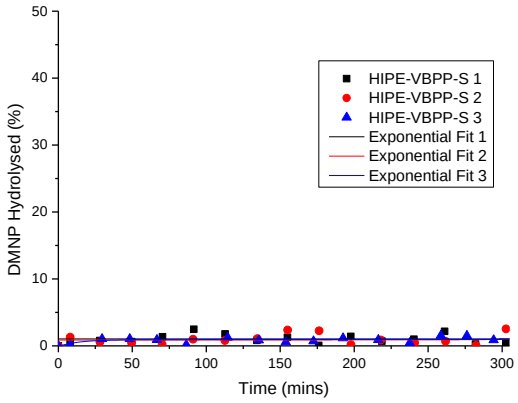

Figure S15. A plot showing the hydrolysis of DMNP over time in the presence of HIPE-VBPP and 0.45 M NEM buffer, THF and H_2O. The individual data points for each data set in a triplicate are shown, along with the exponential fit that was derived from each data set.

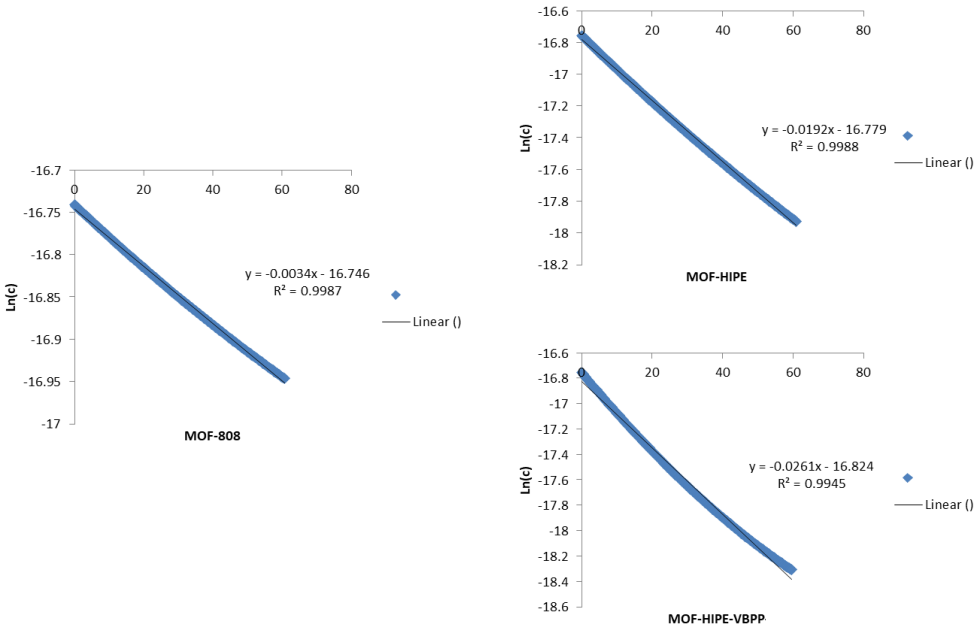

Figure S16. Natural logarithms of concentrations corresponding to DMNP residues in the presence of MOF-808 and the MOF/HIPE composites. The first order rate constants were calculated from a linear fit through the initial data points (first 60 minutes) for each composite.

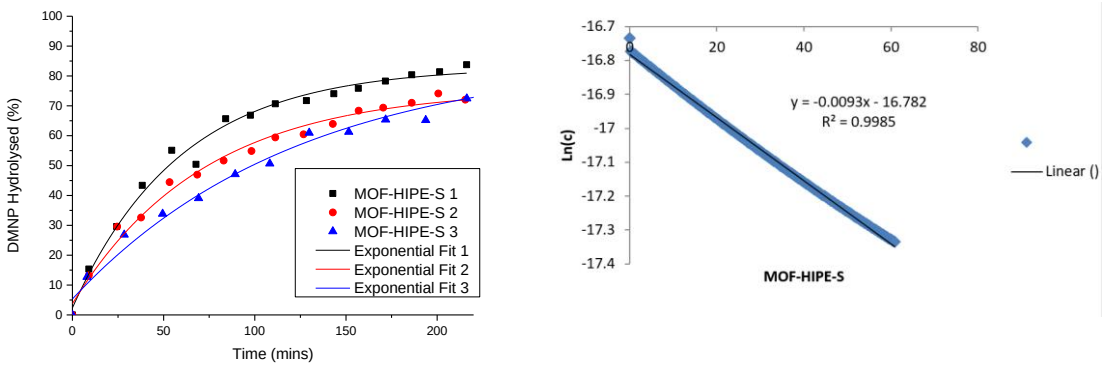

Figure S17. Left. A plot showing the hydrolysis of DMNP over time in the presence of MOF-HIPE and H_2O. The individual data points for each data set in a triplicate are shown, along with the exponential fit that was derived from each data set. **Right**. Natural logarithms of concentrations corresponding to DMNP residues in the presence of MOF-HIPE. The first order rate constants was calculated from a linear fit through the initial data points (first 60 minutes).

DMNP hydrolysis throughout sections of MOF-HIPE

The following procedure was used to observe the difference in hydrolysis between different sections of MOF-HIPE. DMNP 120 µL (0.54 mmol) was dissolved in a solution of 2.4 ml of D_2O, 2.4 ml THF and 2.4ml of 1.45 M NEM aqueous buffer (effective concentration 0.45 M), the solution was transferred to a petri dish. A single circular chunk of MOF-HIPE 200 mg (40 mg, 1.37 µmol, 2.5 mol %) was placed in the centre of the dish with roughly half of the polymer being above the solution level. The reaction was covered and left for 3 hours. After 3 hours, the polymer was removed from the dish, a circular segment was then cut from the central half of the HIPE thus also leaving a circular outer half. The contents of the central half (Section 2) were vacuum filtered and analysed using ^{31}P NMR spectroscopy. The contents of the outer half (Section 1) were also vacuum filtered and analysed using ^{31}P NMR spectroscopy. Finally, an aliquot was taken from the remaining reaction mixture and analysed using ^{31}P NMR spectroscopy (Figure S19).

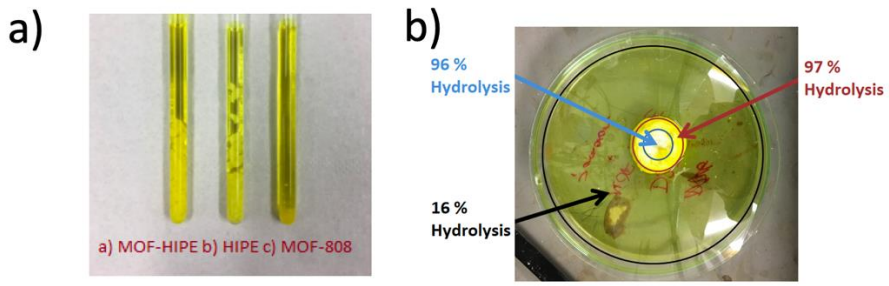

Figure S18. In-composite hydrolysis studies: **a)** An image highlighting the difference in dispersion of MOF-808. Both tube a) and c) contain the same quantity of MOF. Tube a) shows the superior dispersion provided by the HIPE polymer matrix; **b)** An image showing a DMNP degradation mixture containing MOF-HIPE, 2 different sections of the composite were analysed for their degradant composition after 3 hours, both sections exhibited a similarly high degree of DMNP hydrolysis. Only 18 % hydrolysis was observed in the supernatant.

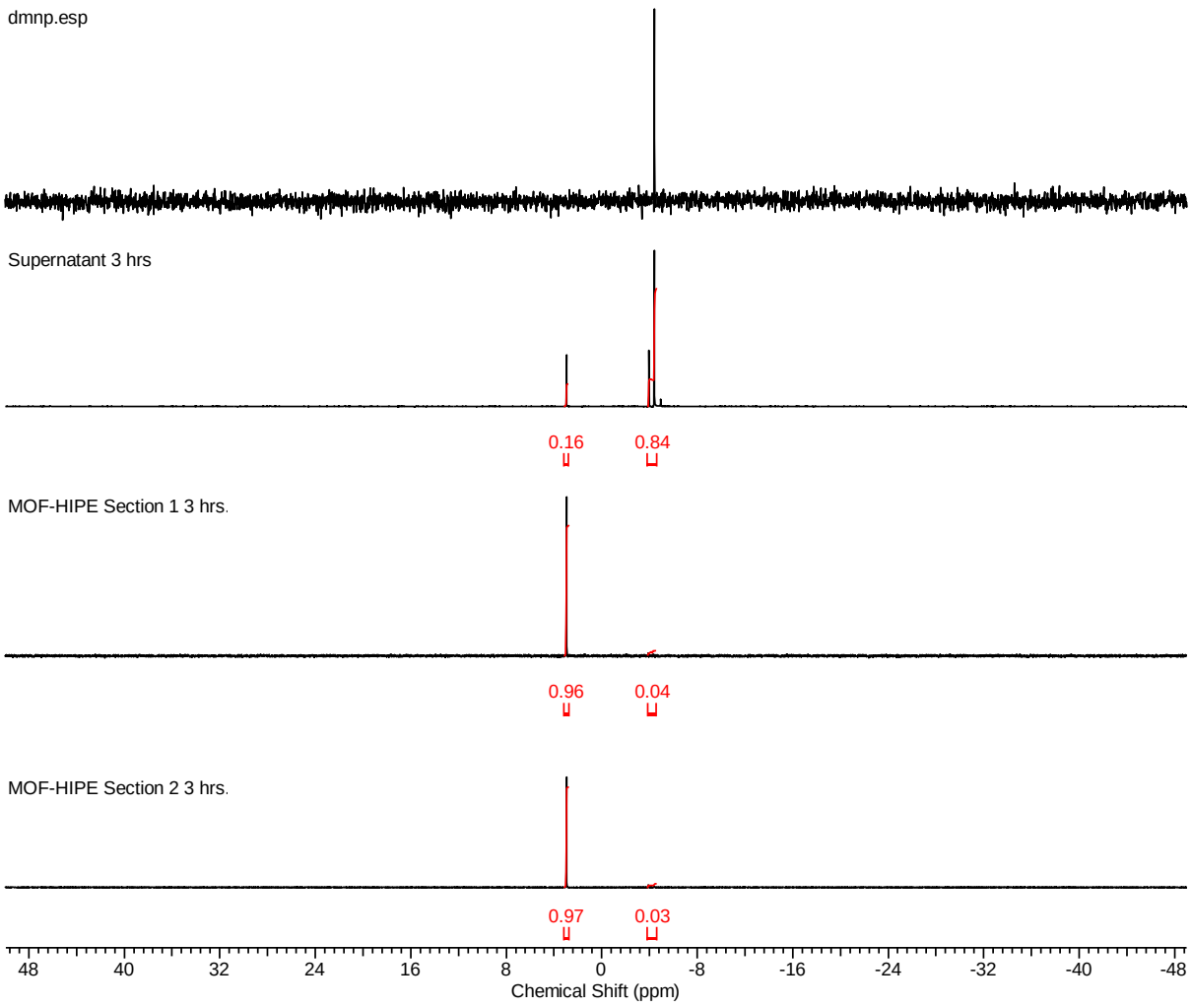

Figure S19. A ^{31}P NMR in D_2O showing aliquots of DMNP taken from 3 different sections (Supernatant, Section 1 and Section 2) of a 0.45 M NEM buffered reaction mixture, containing MOF-HIPE, after 3 hours. The peak at -4.4 pmm is DMNP, the peak at 2.8 ppm is DMP, the DMNP hydrolysis product.

MOF-HIPE Hydrolysis Cycling

The following procedure was used to test the hydrolytic effectiveness of MOF-HIPE-S over 3 cycles. The HIPE containing MOF-808 (3.2 mg, 0.11 µmol, 1.25 mol %) was sliced up into small chunks (1-2 mm^3) then added to the tube along with 0.6 ml mixture containing: 0.2 ml of D_2O, 0.2 THF and 0.2 ml of 1.45 M *N*-ethyl morpholine (NEM) aqueous buffer (effective concentration 0.45M). The tube was inverted once and left to stand for 24 hours at room temperature (298 K). After 24 hours, the tube was analysed using ^{31}P NMR spectroscopy. The HIPE was then removed from the tube, washed 5

times with THF and re-used in the same manner as described above. This was repeated two more times to give a total of 3 cycles (Figure S20).

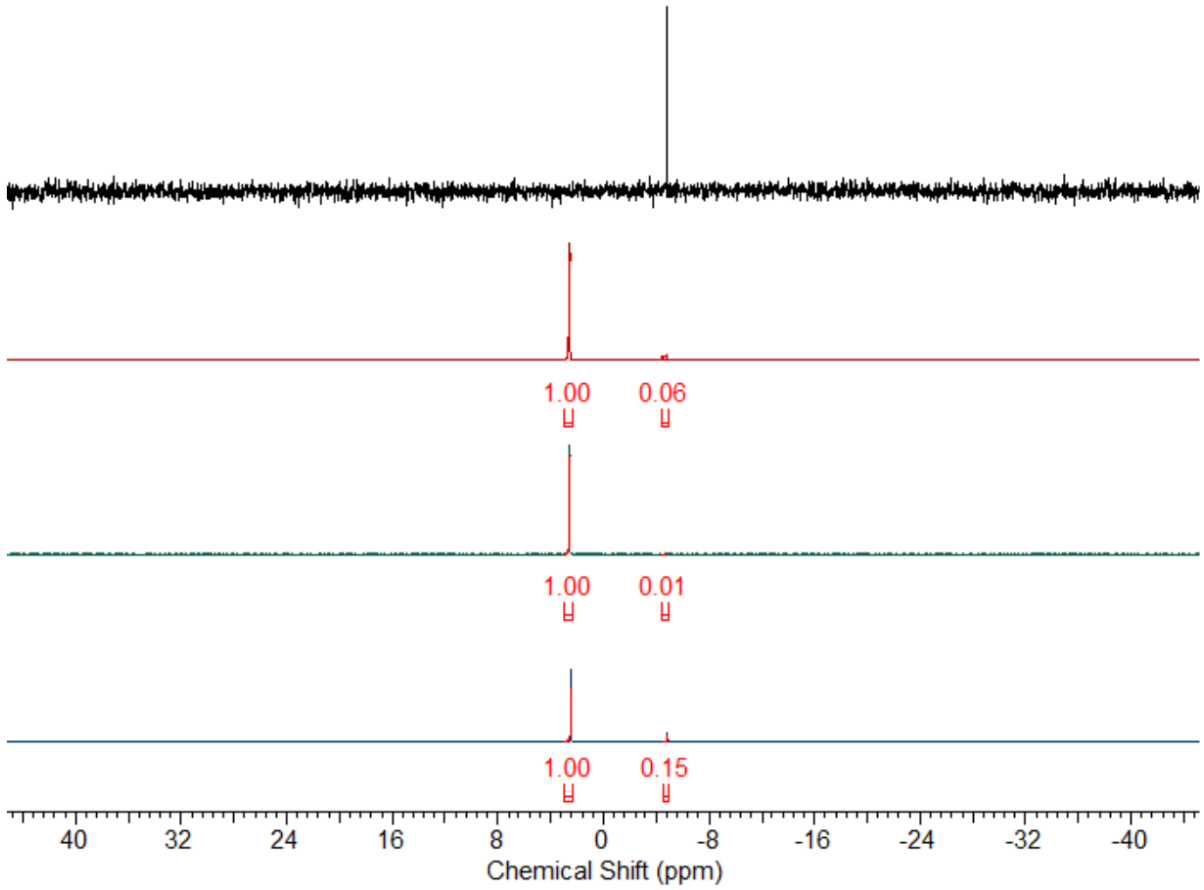

Figure S20. A ^{31}P NMR in D_2O overlay showing (black) fresh DMNP (red; cycle 1) DMNP 24 hours after the addition of MOF-HIPE containing 1.25 mol % MOF-808 relative to substrate in 0.45 M NEM buffer (green; cycle 2) DMNP 24 hours after the addition of the same MOF-HIPE-S containing 1.25 mol % MOF-808 relative to substrate in 0.45 M NEM buffer (blue; cycle 3) DMNP 24 hours after the addition of the same MOF-HIPE containing 1.25 mol % MOF-808 relative to substrate in 0.45 M NEM buffer. The peak at -4.4 pmm is DMNP, the peak at 2.8 ppm is DMP, the DMNP hydrolysis product.

Non-Buffered DMNP hydrolysis procedure

The following procedure was used to probe the hydrolysis rates of the MOF-HIPE-VBPP-S polymer composite material using a non-buffered simulant screening system. 5 NMR tubes were each charged with DMNP, 5 µL (0.02 mmol). HIPEs were all sliced up into small chunks (1-2 mm^3). Various quantities of MOF-HIPE-VBPP (Table S5) were used (32.5mg, 16.5 mg and 8 mg) along with MOF-HIPE (32.5 mg) and MOF-808 (5.2 mg). (2.7 mg, 0.09 µmol, 7.3 %) and 4-vinylbenzyl piperidine. MOF-HIPE-VBPP-S (8 mg) contained MOF-808 (1.3 mg, 0.04 µmol, 3.6 mol %) and 4-vinylbenzyl piperidine. For controls, MOF-HIPE-S (32.5 mg) was used which contained MOF-808 (5.2 mg, 0.18 µmol, 14.5 mol %) and powdered MOF-808 (5.2 mg, 0.18 µmol, 14.5 mol %). Each quantity of HIPE was sliced up into small chunks (1-2 mm^3) then added to the corresponding tube along with 0.2 ml of D_2O, 0.2 THF and 0.2 ml of H_2O. The tubes were inverted once and left to react for 20 hours. After 20 hours, the content of each tube was analysed using ^{31}P NMR spectroscopy (Figure S21).

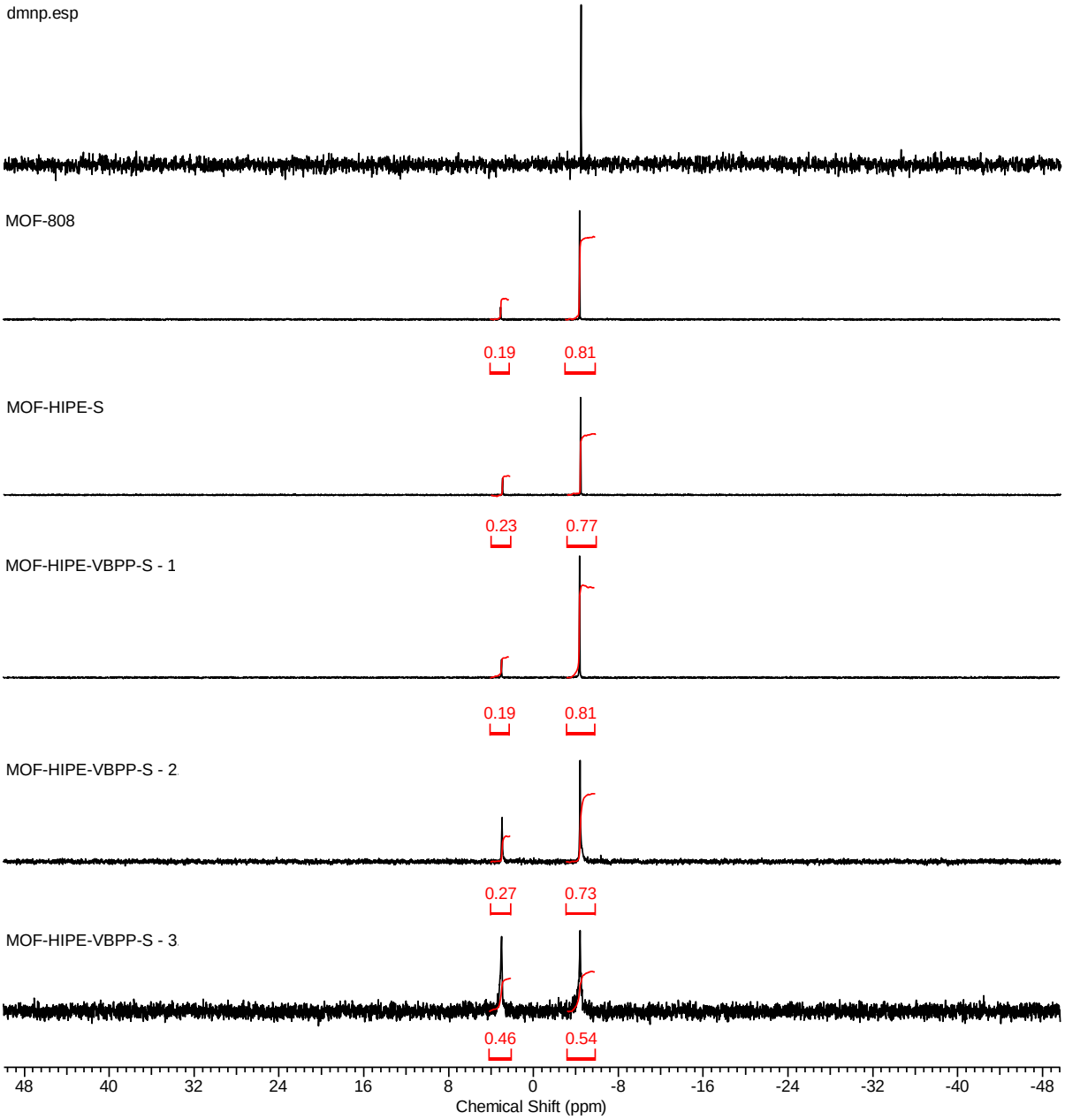

Figure S21. A ^{31}P NMR overlay showing DMNP in D_2O/THF 20 hours after the addition of a corresponding composite/control material in the absence of buffer. The peak at -4.4 pmm is DMNP, the peak at 2.8 ppm is DMP, the DMNP hydrolysis product.

Table S5. A table showing the various quantities of MOF-HIPE-VBPP-S that were screened on DMNP in the absence of any NEM buffer and the degree of hydrolysis that was observed. MOF-HIPE-S and MOF-808 were included as blanks.

Sample + Quantity	**MOF-808 quantity**	**4-VBPP : DMNP Ratio**	**% DMNP Hydrolysed after 20 hours**
MOF-HIPE-VBPP 3 32.5 mg	4.9 mg	1:4	46.0 %
MOF-HIPE-VBPP 2 16 mg	2.4 mg	1:8	27.0 %
MOF-HIPE-VBPP 1 8 mg	1.2 mg	1:16	19.0 %
MOF-HIPE 32.5 mg	4.9 mg	No 4-VBPP	23.0 %
MOF-808 4.9 mg	4.9 mg	No 4-VBPP	19.0 %

Section 4: VX Hydrolysis Studies

VX hydrolysis procedure in the presence of Water/THF (performed by Dstl)

The following procedure was used to probe the hydrolysis rates of the various MOF and polymer composite materials for the degradation of VX in a mixture of THF and water. The HIPE containing MOF-808 (3.2 mg, 0.11 µmol, 1.25 mol %) was sliced up into small chunks (1-2 mm^3) then added to an NMR tube along with VX, 24 µL (0.09 mmol). A 0.6 ml mixture containing: 0.15 ml of D_2O, 0.3 ml of THF and 0.15 ml of H_2 was then added. The tube was inverted once and immediately loaded into an NMR auto-sampler and the first spectrum was obtained within 8 minutes of the reaction commencing. The sample was then cycled on the auto-sampler to collect subsequent data points. Each measurement was performed once (Figure S22-23).

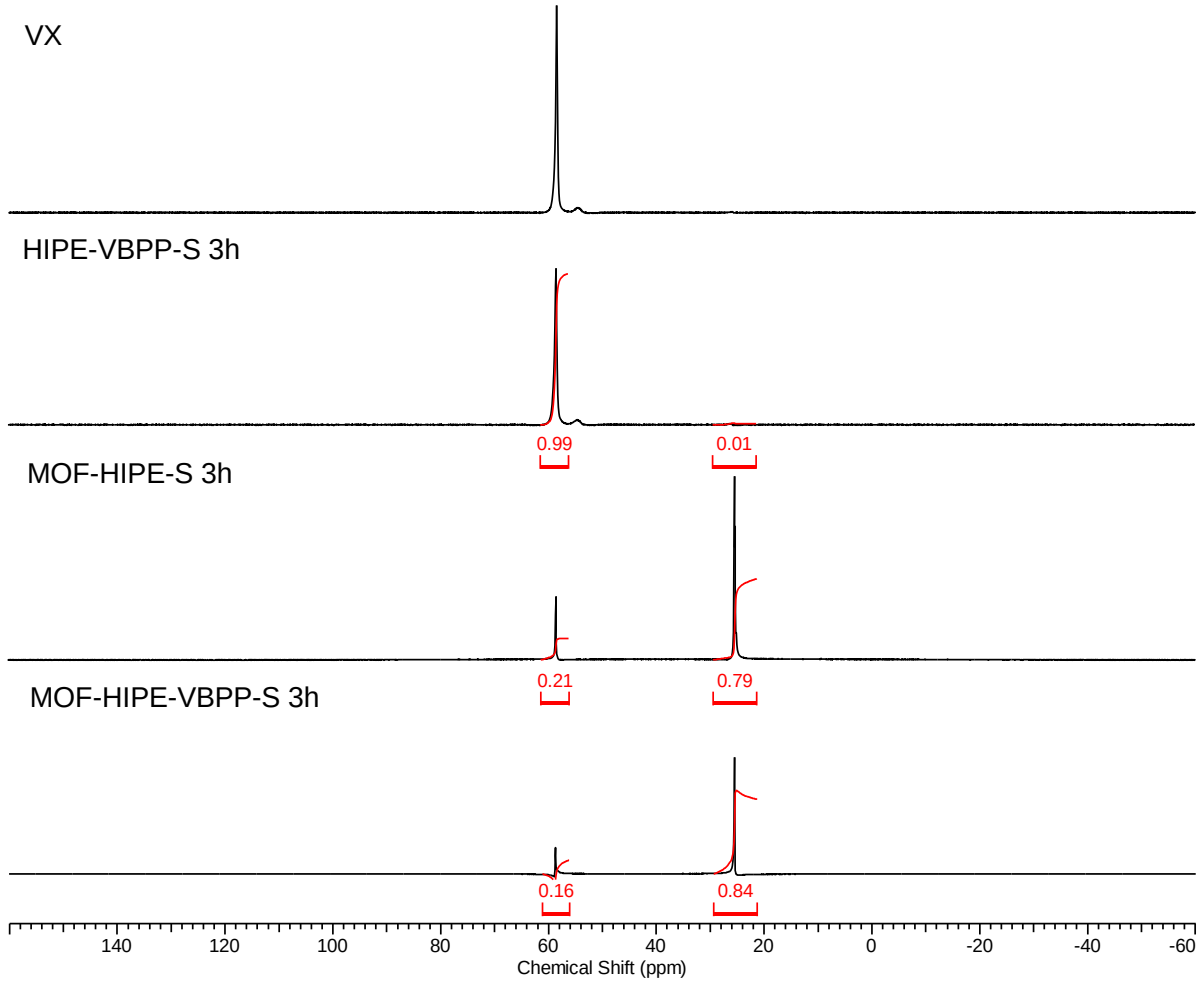

Figure S22. A ^{31}P NMR in D_2O/THF overlay showing VX 3 hours after the addition of a corresponding composite/control material. The peak at 58.6 pmm is VX, the peak at 25.4 ppm is EMPA, the VX hydrolysis product.

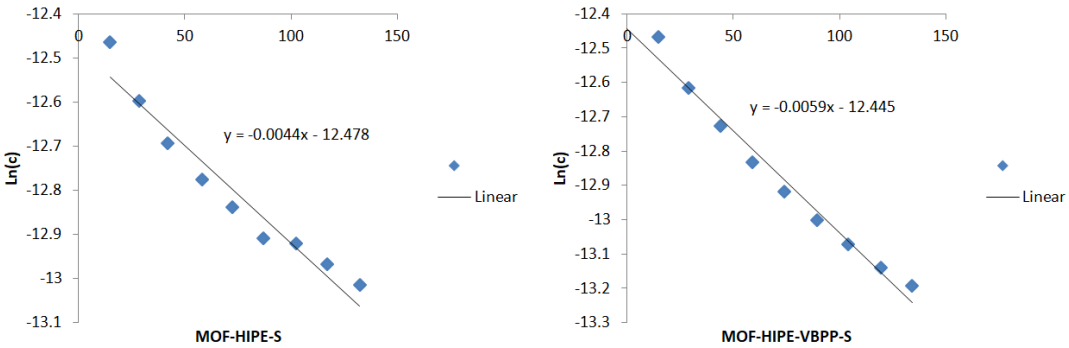

Figure S23. Natural logarithms of concentrations corresponding to VX residues in the presence of MOF-HIPE-VBPP and MOF-HIPE. The first order rate constants were calculated from a linear fit through the initial data points (first 120 minutes) for each composite.

Neat VX hydrolysis procedure (performed by Dstl)

The following procedure was used to probe the hydrolysis rates of the various MOF and polymer composite materials for the degradation of neat VX in absence of solvent and buffer. A vial was charged with VX (267.37 g/mol, 250 uL, 1.14 mmol) and The HIPE (10mg) containing MOF-808 (2 mg, 0.15 mol %), the ambient humidity was recorded (50 RH %). A small aliquot was taken after 4d, 7d, 11d and 14d and analysed using ^{31}P NMR spectroscopy. Each measurement was performed in duplicate (Figure S24)

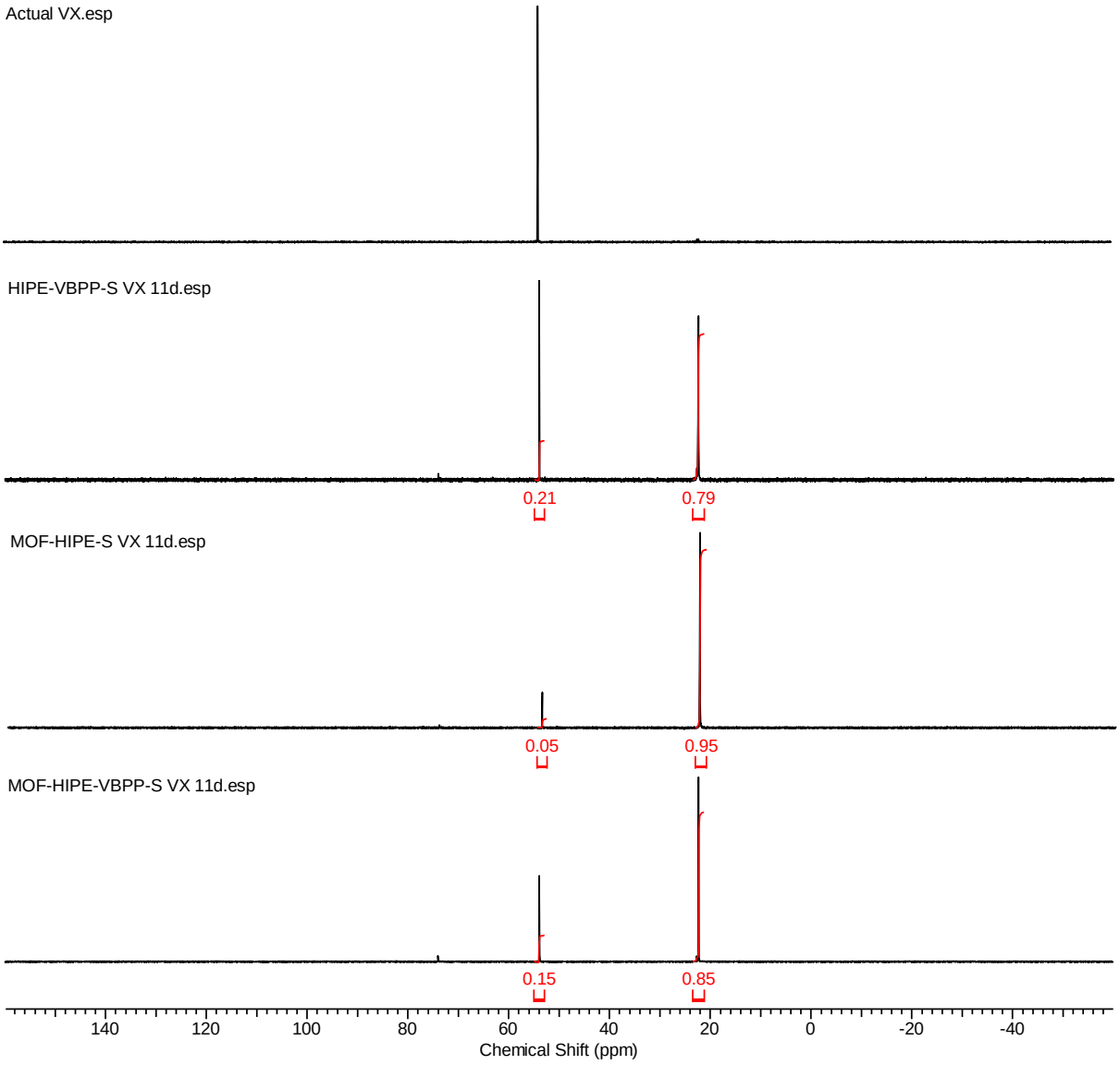

Figure S24. A ^{31}P NMR in $CDCl_3$ of an aliquot of VX taken from a corresponding material after 11 days in the presence of 50 % relative humidity. The peak at 58.6 pmm is VX, the peak at 25.4 ppm is EMPA, the VX hydrolysis product.